



UNIVERSITÄT FÜR BODENKULTUR WIEN
University of Natural Resources
and Life Sciences, Vienna

Master Thesis

The development of *Dicranopteris* in Costa Rican secondary rainforests and its impact on tree development

submitted by

Stephan Alexander GRÄBER, BSc

in the framework of the Master programme

Forstwissenschaften

In partial fulfilment of the requirements for the academic degree

Diplom-Ingenieur

Vienna, March 2023

Supervisor:

Univ.Prof Mag. Dr. Peter Hietz
Institute of Botany
Department of Integrative Biology and
Biodiversity Research (DIB)

Co-Supervisor:

Dipl.-Ing. Dr. Markus Immitzer, MSc.
Institute of Geomatics
Department of Landscape, Spatial and
Infrastructure Sciences

Abstract

Forests and trees can experience rapid growth in tropical climate, leading to the fixation of large quantities of CO₂ out of the atmosphere when compared to other regions. Hence, the protection of existing rainforests as well as converting unforested land into forests are measures to address climate change and its impact. Tropical secondary forests in the vicinity of La Gamba have been shown to recover rapidly. However, the recovery rates might be biased and too optimistic if only areas with well-functioning regeneration are being looked at. On several deforested sites in Costa Rica a fern (*Dicranopteris*) has established. *Dicranopteris* is distributed pantropically and is known to form vast, dense monospecific stands that can persist for a long period of time, impeding the succession of trees and therefore leading to major delays in the trees' development.

This study aims to characterize the development of fern-dominated sites in the vicinity of the Tropical Field Station La Gamba. 23 plots were investigated using aerial photography, drone and satellite images of different years. Their size was determined, and satellite images were semi-automatically classified. In the vicinity of La Gamba *Dicranopteris* covers > 1 % of the area and was shown to arrest succession for at least 49 years on one site. During the past seven years, little if any of these areas converted to forests, resulting in reduced carbon sequestration. The results show that regeneration of tropical forests can be too optimistic. Options for managing fern thickets in the vicinity of La Gamba are discussed.

Keywords: *Dicranopteris*, arrested succession, forest degradation, remote sensing

Zusammenfassung

Wälder und Bäume können in tropischem Klima schnell wachsen, was dazu führt, dass sie im Vergleich zu anderen Regionen große Mengen CO₂ aus der Atmosphäre binden. Daher sind der Schutz der bestehenden Regenwälder und die Umwandlung von unbewaldeten Flächen in Wald vielversprechende Maßnahmen zur Bekämpfung des Klimawandels und seiner Auswirkungen. Tropische Sekundärwälder in der Umgebung von La Gamba können sich schnell erholen. Allerdings könnten die Erholungsraten verzerrt und zu optimistisch sein, wenn nur Gebiete mit gut funktionierender Regeneration betrachtet werden. An mehreren entwaldeten Standorten in Costa Rica hat sich der Farn *Dicranopteris* etabliert. *Dicranopteris* ist pantropisch verbreitet und dafür bekannt ausgedehnte, dichte Reinbestände zu bilden, die über einen langen Zeitraum bestehen bleiben können. Das behindert die Sukzession von Bäumen und kann somit zu erheblichen Verzögerungen in der Entwicklung der Bäume führen.

Ziel der Arbeit ist, die Entwicklung von farndominierten Standorten in der Umgebung der Tropenstation La Gamba zu charakterisieren. 23 Flächen wurden anhand von Luftaufnahmen, Drohnenbildern und Satellitenbildern aus verschiedenen Jahren untersucht. Die Größe der Farnbestände wurde erfasst, und die Satellitenbilder wurden halbautomatisch klassifiziert. In der Umgebung von La Gamba bedeckt der Farn > 1 % der Fläche. An zumindest einem Standort blockiert *Dicranopteris* die Waldsukzession mindestens 49 Jahre lang. In den letzten sieben Jahren sind Farnbestände kaum von Wäldern ersetzt worden, womit sie eine entsprechend reduzierte C-Senke darstellen. Die Ergebnisse zeigen, dass die Regeneration von tropischen Sekundärwäldern zu optimistisch sein kann, und verdeutlichen den Handlungsbedarf bei der Bekämpfung von Farnflächen in der Umgebung von La Gamba.

Stichworte: *Dicranopteris*, gehemmte Sukzession, degradierte Wälder, Fernerkundung

Table of Contents

1. Introduction	1
1.1 Importance of tropical rainforests and their threats.....	1
1.2 Successional trajectories	3
1.3 A fern arresting succession	5
1.4 Potential of remote sensing in environmental research	7
1.5 Aims & Hypotheses.....	9
2. Material and methods	10
2.1 Study area and plot selection	10
2.2 Tree measurements	11
2.3 Drone image acquisition.....	12
2.4 Drone image processing	14
2.5 Area assessment of fern-dominated sites	14
2.6 Canopy cover.....	15
2.7 Satellite image acquisition and processing.....	15
2.8 Aerial photograph evaluation.....	16
2.9 Semi-automatic area assessment	17
3. Results	20
3.1 Tree circumference measurements.....	20
3.3 Manual area assessment based on drone and Planet data from 2022	21
3.4 Semi-automatic classification of Planet data of 2022	22
3.5 Fern detection based on Planet data of 2017	24
3.6 Fern detection based on Pléiades data of 2015	26
3.7 Evaluation of aerial photography of different time steps	28
3.8 Comparison of assessed area.....	30
4. Discussion	34
4.1 Correlating DBH and crown area	34
4.2 Drone campaign.....	35
4.3 Fern-dominated area assessment.....	36
4.4 <i>Dicranopteris</i> development	37
4.5 Biomass accumulation	39
4.6 Conclusion.....	41
Acknowledgements.....	42
Image References	43
References	44
Appendix.....	54

1. Introduction

1.1 Importance of tropical rainforests and their threats

Tropical rainforests are the terrestrial ecosystems with the highest biodiversity (Kricher 2011). Holding just 6 % of global area, they are estimated to host around two thirds of the world's vascular plants species thus sparking the interest of researchers and tourists alike (Turner 2001; Corlett and Primack 2011). If only trees are looked at, the share of species located in the tropics is even higher (Schultz 2000; Poorter L et al. 2015). Furthermore, they are also the home of many indigenous people (Zaman 2022). The forests of the neotropics are especially diverse. The ratio of plant species richness is around 3 : 2 : 1 when compared to the Asian-pacific and African rainforests (Corlett and Primack 2011). Although Costa Rica is a small country, making up 0.03 % of the earth's landmass, it hosts around 5 % of the estimated worldwide species (Johnston 2022). Especially Costa Rica's Golfo Dulce region has a high botanical diversity harbouring more than 2,300 species of vascular plants (Weissenhofer et al. 2001).

Tropical forests have by far the highest share of forest ecosystems with 45 % of forests being in the tropics followed by boreal forests with 27 % and temperate and subtropical forests with 16 and 11 % respectively (FAO 2020). Furthermore, tropical rainforests have the highest annual net primary productivity of all terrestrial systems (Kricher 2011). Being the largest terrestrial carbon sink, they play a vital role in reducing climate change (Phillips et al. 1998; Anderson-Teixeira et al. 2016).

Unfortunately, the diversity, spatial extent and role as a carbon sink of tropical rainforests are threatened. The yearly deforestation rate in the tropics in the period between 2015 and 2020 was 9.3 million ha (FAO 2020). Although the rate has been decreasing since 1990, it is still the yearly equivalent of an area 1.8 times the size of Costa Rica. Even when comparing these numbers to other climatic domains, they remain inarguably high. For example, the deforestation rate in the subtropics, which is the second highest, is much lower with 0.5 million ha per year (FAO 2020). Deforestation can have detrimental effects on a global and local scale. Surface temperatures can increase by 1 - 3 K locally, rainfall can decrease by 40%, biodiversity can decline, and scores of people can lose their home (Bennet 2017; McFarland 2018; Spracklen et al. 2018; Lo et al. 2020). While deforestation has strong negative effects, forest

degradation also impacts ecosystem functions and services. Some even argue that it is a more serious problem than deforestation (FAO 2002a). Houghton (2012) estimated that degradation amounted to 10 – 40 % of the yearly ~ 1.4 Pg C emissions of tropical deforestation and degradation between 1990 and 2010. The uncertainty in these numbers stem from the difficulty in documentation and varying definitions of the term. On top of carbon emissions, forest degradation leads to biodiversity loss and decrease of ecosystem services (Ghazoul et al. 2015; FAO 2020). Yet, there is still no widely applied definition for forest degradation which is likely to increase (FAO 2022). The FAO (2002b) defines forest degradation as “the reduction of the capacity of a forest to provide goods and services”. While this definition is often used, critics say it takes too little notice of resilience, is too broad and may therefore be adapted to suit local management or policy context (Ghazoul et al. 2015). For instance, a reference state could be used that is not realistic to mask bad management practices and their resulting C emissions. Drivers of tropical deforestation differ among regions (Fig. 1), however the biggest carbon source in relation to deforestation and forest degradation in Latin America is agriculture, in particular shifting cultivation (Houghton 2012; McFarland 2018).

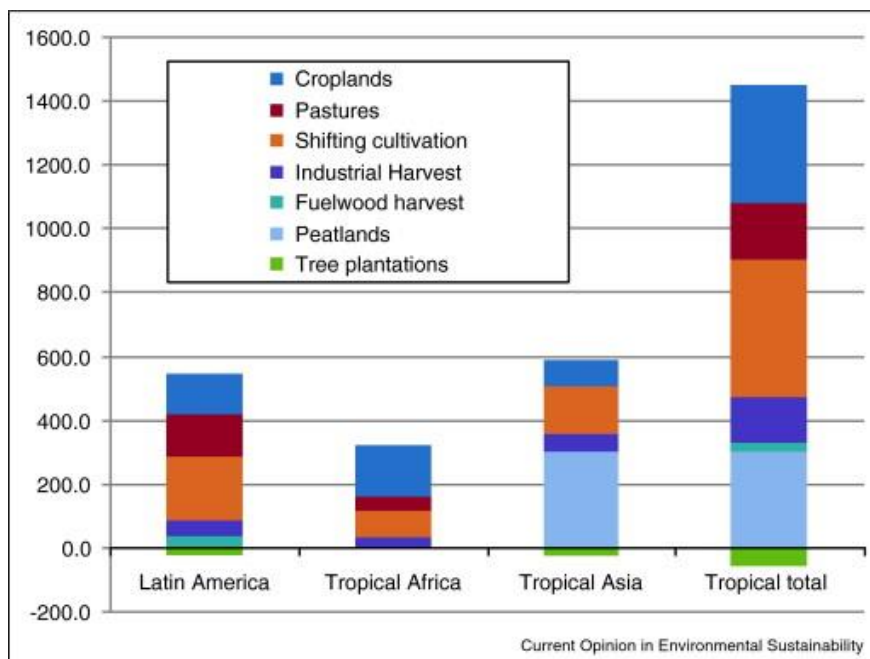


Figure 1: Sources (+) and sinks (-) of carbon (TgC yr⁻¹) from activities contributing to deforestation and forest degradation in tropical regions. Source: Houghton (2012)

Reforestation projects can work against the aforementioned effects (Chazdon et al. 2016). While reforestation in Europe is often primarily driven by economical purposes such as timber production, the incentive often differs in the tropics. These projects

usually have one main objective that should be tackled, however in doing so they impact others, too (Fagan et al. 2016). For example, a reforestation project aimed at creating a habitat would re-establish some of the hydrological processes and store carbon at the same time (Lamb 2011). Reforestation can help mitigate climate change through an array of means like carbon storage, surface roughness and evaporation (Locatelli et al. 2015). One such project is the Corredor Biológico de La Gamba (COBIGA) in south-western Costa Rica. It aims to improve habitat connectivity of animals and plants by connecting the low land forests of the Piedras Blancas national park in the Golfo Dulce region with the montane forests of the Fila Cal (Weissenhofer et al. 2016). The COBIGA project is managed by the Tropical Field Station La Gamba which was founded by the University of Vienna and the foundation “Regenwald der Österreicher” (Engl.: Rainforest of the Austrians, Span: Bosque de los Austríacos). In collaboration with COBIGA, the recovery and restoration of the local rainforest is studied. Oberleitner et al. (2021) found fast regeneration of secondary forests in the area of La Gamba. A key finding is that within around 20 years, species richness can regenerate to 31 % and aboveground biomass (AGB) to 52 % to that of an old growth forest. Other studies from the neotropics showed similar results, supporting the potentially rapid regeneration of rainforests (Letcher and Chazdon 2009; Poorter et al. 2016). However, these results might be biased and too optimistic if only areas with well-functioning regeneration are being looked at.

1.2 Successional trajectories

Ecological succession (hereon after succession) can be defined as the “replacement of an organism community by another, led by climate, soil or through the organisms themselves” (Schaefer 2012). It can further be distinguished between primary succession, that describes the dynamics following the establishment of the very first organisms on the site, for example on newly formed islands; and secondary succession (Kratohwil and Schwabe 2001). The latter describes the dynamics after a disturbance, like a clear-cut. Succession is often portrayed to follow a predictable pathway of establishing species or species communities (Finegan 1996; Kratohwil and Schwabe 2001; Chapin et al. 2002; Kricher 2011). While this might be accurate in many cases, it does not always occur in such a linear way. Instead, understory layers can exclude tree recruitment for a prolonged time (Royo and Carson 2006). This has been described as retarded succession (Kuroda et al. 2006), delayed succession, or

arrested succession (Royo and Carson 2006; Goldsmith et al. 2011). There is no generally accepted term for this phenomenon as some call any state of such kind ‘arrested’ (Kricher 2011). Thrippleton et al. (2018) point out the importance of a clear definition for such a state and acknowledge the distinction between ‘delayed succession’ and ‘arrested succession’ discussed by Royo and Carson (2006), depending on the persistence of the state. However, they criticise the lacking time domain in the definitions and suggest using ‘delayed succession’ for decadal time scales and ‘arrested succession’ for centennial time scales. Yet, proving a case of arrested succession might be difficult using this definition as extensive knowledge of the particular site is required that can only be acquired through specialized methods like pollen analysis (i.e. Kneller 2009).

Ghazoul and Chazdon (2017) define a ‘persistent state’ as: “a temporarily stable ecosystem over discrete spatial scales, which shifts to alternative states subject to natural dynamics and disturbances” and ‘arrested succession’ as: “an ecosystem state in which dynamics are halted such that continued recovery is not possible without human intervention”. Since such a state is more easily proven, while implying that ‘arrested succession’ is a more severe case of a persistent state, this definition will be used in the present study.

Persistent states have been described for different sized organisms in various locations with varying underlying mechanisms. For instance, persistent dominance by grasses have been described for boreal systems and Uganda (Royo and Carson 2006; Wheeler et al. 2016), and persistent shrub states for Spain, Portugal and boreal regions (Royo and Carson 2006; Acácio et al. 2007; DeSoto et al. 2010). In the tropics and subtropics, cases of persistent dominance by ferns (Levy-Tacher et al. 2015), bamboo (Kellermann and Lacerda 2019) and trees (Boyes et al. 2011) have been documented. Royo and Carson (2006) describe six mechanisms that either individually or combined can lead to persistent states and arrested succession. These are above- (1) and below-ground competition (2), allelopathy (3), seed and (or) seedling predation (4), litter accumulation (5) and mechanical damage (6).

1.3 A fern arresting succession

Dicranopteris is a fern genus distributed throughout the subtropics and tropics (Zhao et al. 2012; Yang L et al. 2020). Members of this genus often colonize anthropogenically degraded sites like abandoned pastures (Schnetzer 2014), burned sites (Shono et al. 2007), abandoned agricultural sites (Ashton et al. 2001), abandoned mining sites (Jally et al. 2021), roadsides (Dos Santos et al. 2010; Lima et al. 2021) and clear cut forests (Yamagawa et al. 2010). They are also common on naturally poor soils and disturbed sites like lava flows (Hughes et al. 2014), open forests (Vitousek et al. 2010; Mueller-Dombois and Boehmer 2013) and land-slides (Walker et al. 2010).



Figure 2: *Dicranopteris pectinata* thicket with characteristic litter layer in the foreground and climbing ability in the centre and on the right in the background.

These sites are all very light exposed, highlighting that *Dicranopteris* is photophilous (Holttum 1959). *Dicranopteris* can form dense thickets that are often monospecific or contain only a few shrubs and trees (Underwood 1907; Walker 1994; Russell et al. 1998; Slocum et al. 2004). This is at least partly owed to its ability of reproducing vegetatively (Russell et al. 1998). *Dicranopteris*' creeping rhizomes and indefinite growth of fronds lead to it being able to cover large areas (Holttum 1959). Stands formed by members of this genus can extend over hundreds of acres (MacCaughey 1918) and persist for a long time (Holttum 1959; Russell et al. 1998). Several mechanisms lead to the dominance of members of this genus. Firstly, their high water and

phosphorus use efficiency is an important adaptation to colonize sites that provide extreme conditions for others (Holtum 1959; Russell and Vitousek 1997; Russell et al. 1998; Yang L et al. 2020). The ability to reproduce clonally allows them to colonize adjacent sites rapidly after a clearing presented itself (Walker and Boneta 1995; Slocum et al. 2004; Slocum et al. 2006; Chau and Chu 2017). Soon after colonization, their canopy can shade out possible competitors (Walker 1994). For *Dicranopteris linearis* a relative illuminance level of one percent at the ground level was shown by Kuroda et al. (2006). Similarly, Wyns (2015) found a light reduction at soil level of over 99 % for *D. pectinata*. Dead litter plays an essential role in creating these dark conditions (Ainsworth and Kauffman 2010; Wyns 2015). *Dicranopteris* thickets have been described to consist of three strata: living fronds at the top, dead material in the middle, and the root layer (MacCaughey 1918; Slocum et al. 2004; Slocum et al. 2006). The live and dead material is often very tightly interwoven (MacCaughey 1918). So much so that it can withstand the weight of several men jumping on it without touching the ground (Underwood 1907). It is believed that it can therefore also act as a mechanical barrier that prevents seeds from reaching the floor (Chua et al. 2016). Even if trees can develop on a particular site they might be compromised, as *Dicranopteris linearis* and *D. pectinata* have been described to climb onto trees, potentially smothering them (MacCaughey 1918; Russell et al. 1998; Shiels and Walker 2003; Vitousek et al. 2010). The mechanisms described in this paragraph mainly correspond to aboveground competition, however the change in light regime is also largely impacted by the litter accumulation (Royo and Carson 2006). *Dicranopteris* has also been speculated to have allelopathic properties that promote the persistence (Goldsmith et al. 2011; Yang L et al. 2020). The litter has a high phenolic content which leads to slow decomposition (Russell and Vitousek 1997; Amatangelo and Vitousek 2009). While phenolics often play a role in allelopathy (Tet-Vun and Ismail 2006), they are very common in plants, hence their mere occurrence cannot prove allelopathy (Inderjit and Mallik 2002). Several studies showed evidence of allelopathy for *D. linearis*, *D. pedata*, *D. flexuosa*, and *D. pectinata* (Li-Ping et al. 1999; Tet-Vun and Ismail 2006; Kato-Noguchi et al. 2012; Gul et al. 2019). However, the evidence for *D. pectinata* is not very conclusive as both Walker (1994) and Wyns (2015) could not prove allelopathy for this species. *Dicranopteris pectinata* Underw. (syn. *Gleichenella pectinata* (Willd.) Ching) and *Dicranopteris flexuosa* (Schrad.) Underw. are the



only two members of this genus native to Costa Rica (POWO 2022). The former seems to be more common around the Tropical Field Station. Its distribution ranges from northern Mexico to Uruguay (Figure 3).

Figure 3: Distribution of *Dicranopteris pectinata*. Adapted from POWO (2022).

While some studies portray *Dicranopteris* to only occur for a shorter period, i.e. “several years” (Dos Santos et al. 2010), most recognize it being dominant for decades or even centuries (Walker 1994; Shono et al. 2006; Shono et al. 2007; Walker et al. 2010; Martin et al. 2011; Crausbay and Martin 2016). Though, there is often no evidence on which the authors base these claims. Based on chronosequencing, Kitayama et al. (1995) estimated it being dominant for 300 years in one case. Another approach to find out *Dicranopteris*’ persistence could come by comparing remote sensing data from different points in time.

1.4 Potential of remote sensing in environmental research

Remote sensing is used in an array of fields including agriculture, forestry, geography, weather, and climate and many more (Chandra and Ghosh 2006; Liang 2012; Rees 2013). The large archive of satellite images, dating back to the 70’s of the last century, allows for monitoring sites over a large period of time (Mitchell et al. 2017). However, some of these sensors, such as Landsat-1, have a coarse spatial resolution (SR) with 80 m (MacDonald 1998). In contrast, civilian satellites today have a SR of up to 0.3 m (Heipke et al. 2017). Based on remote sensing data in combination with field surveys, estimates for the state of forests such as carbon stocks, above ground biomass, and forest structure are possible (Mitchell et al. 2017).

In recent years, unmanned aerial vehicles (hereon after ‘drones’) have proved to be a quick, precise and cost-efficient tool to digitally capture the earth (Resnik and Bill 2009). Additionally, given their low maximum altitude, they provide a very high SR and are less affected by clouds than sensors at higher altitudes (Mitchell et al. 2017). In remote sensing small drones with a maximum weight of 25 kg are commonly used (Heipke et al. 2017). Recent studies show the vast potential drones can have in monitoring plant structural parameters. For instance, Salim et al. (2020) used drones to estimate the biomass of mangrove forests. The biomass estimation based on drone imagery of McCann et al. (2022) in arid areas even proved to be more precise than other, more common measures. Based on a combination of drone imagery, satellite imagery and classification, Takeshige et al. (2022) mapped out the spatial distribution of *Dicranopteris linearis* and vine thickets in Borneo. This study will use a similar approach to map out the development of *Dicranopteris* thickets in the Golfo Dulce region of Costa Rica.

1.5 Aims & Hypotheses

Dicranopteris can form vast dense, monospecific stands that are easily distinguishable from other forms of vegetation. Little is known about the persistence of this species in the Golfo Dulce region and rarely do other studies look at the development of the thickets. Therefore, this study aims to understand how persistent *Dicranopteris*-dominated thickets are in the vicinity of La Gamba using remote sensing data. Additionally, it aims to find out whether remote sensing data and semi-automatic classifications based on it can be used to estimate the biomass of fern-dominated sites quickly and accurately.

Since forests in non-protected areas are likely to be disturbed, the first hypothesis is that the number of fern-dominated sites will increase. Some studies point out that trees would eventually regain dominance of a site by shading out the ferns. Hence, the second hypothesis is that fern patches decrease in size in the presence of trees over time. Furthermore, the third hypothesis is that fern patches increase in size on sites with no tree canopy, such as agriculturally used land, and grassland.

2. Material and methods

2.1 Study area and plot selection

The field work and drone campaign of this study was conducted between 23.04.2022 and 11.06.2022 in the vicinity of the Tropical Field Station La Gamba. The station is located between the small village of La Gamba and the Piedras Blancas national park in the Golfo Dulce region in southwestern Costa Rica (Figure 5). The region is characterized by high precipitation with an average of around 6000 mm per year between 1998 and 2020 and a dry season between December and March (Figure 4).

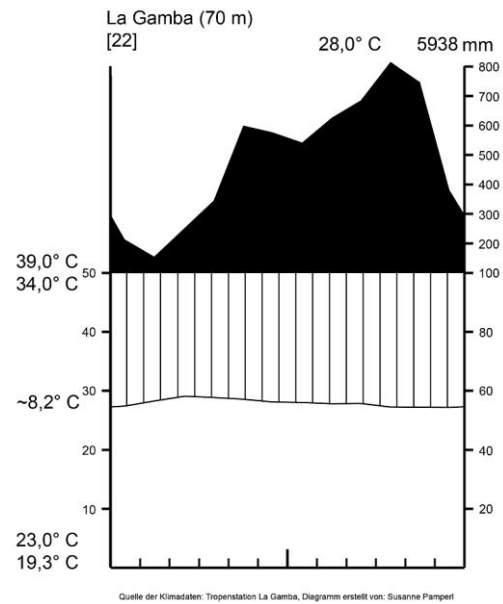


Figure 4: Climate diagram. Source: Tropenstation La Gamba (2020).

Temperatures are tropical with an average of 28° C and the absolute minimum temperature measured between 1998 and 2020 was 19° C.

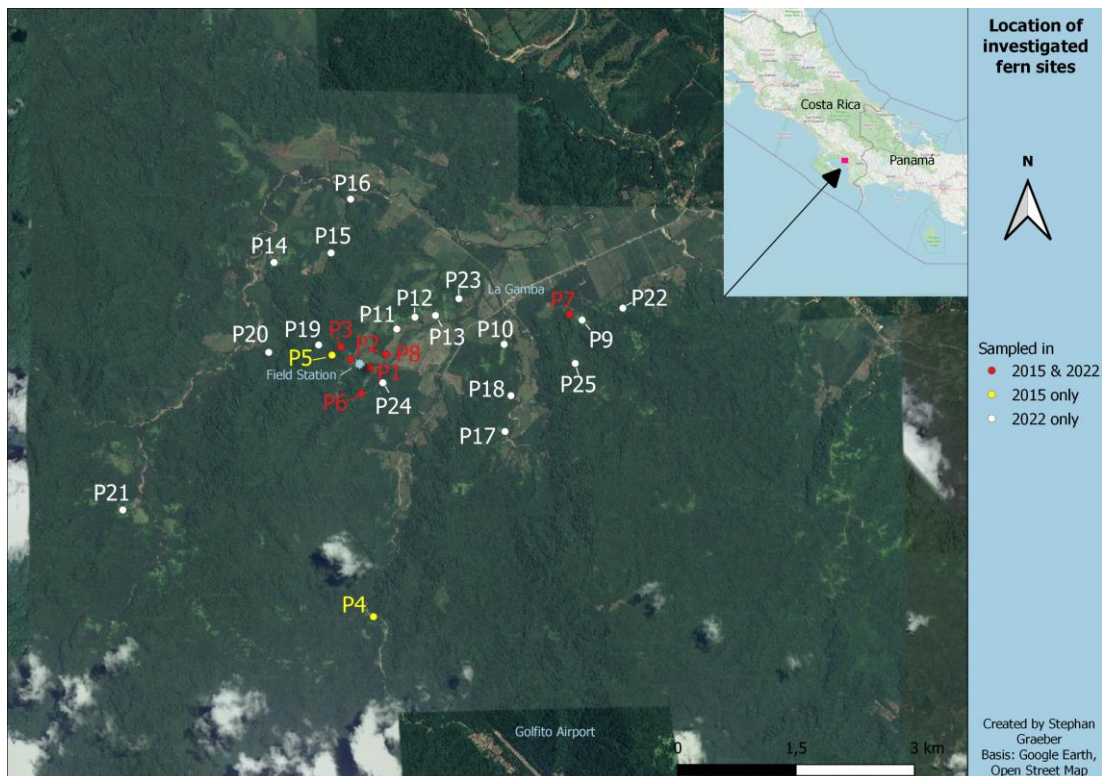


Figure 5: Location of studied plots. Red: Sampled by Wyns (2015) and present study, yellow: sampled by Wyns (2015) only, black: sampled in present study only. Source of base maps: Google Earth (2015). OpenStreetMap contributors (2022).

Wyns (2015) had sampled *D. pectinata* plots around the tropical field station. He selected them for being dominated by the fern and at least 500 m² in size. I aimed to sample the same plots so findings of the present study could be analysed in light of findings of Wyns (2015). All plots sampled in 2015 were visited, however two out of the prior eight studied could not be sampled thoroughly. One did not have an apparent *Dicranopteris* cover. The other was lushly covered by the fern, but drones were not allowed to operate within 3 km of the airport in Golfito.

Seventeen additional plots with a minimum fern cover of around 200 m² were selected. They were chosen by looking at Google Earth imagery as well as riding a bicycle in the area. In total 23 plots were sampled, though this classification stems largely from selection of the starting point of the drone. If it had to be moved in order to fully capture a plot, it was counted as a new plot. The plots were diverse with some consisting of just one fern patch and others consisting of several patches. Also, some plots are directly adjacent to others, while others are further away.

2.2 Tree measurements

On 14 fern-dominated areas the circumference of a number of trees were measured at 1.3 m with a standard measuring tape. However, one plot that was mentioned earlier will not be taken into account in the following as the drone could not take off due to the proximity to the airport (see southern yellow point in Figure 5). Diameter at breast height (DBH) was measured 1.3 m above the ground from a position uphill rather than downhill from the stem. The



Figure 6: Measuring tape and reference stick with red marking.

individuals were chosen for being relatively easy to access, > 11 cm in circumference and surrounded by *D. pectinata*. The species of the measured trees was determined, and notes were taken so that the measured trees could be found on drone images.

2.3 Drone image acquisition



Figure 7: Typical set up before flight: Drone on backpack (foreground), reference stick with red marking on north facing end with a hat and machete underneath the ends of the stick for visibility from above (background).

The DJI Mini 2 drone was used to collect images of the plots. It is equipped with a 12 Megapixel camera (DJI 2021). The drone was launched and landed on a backpack to ensure a level field so rotors would not be damaged, since it does not come with extensive safety features. A wooden stick with a length of 1.74 m was placed on the ground as a size reference and positioned to point north when possible.

This was not always possible due to visibility obstructions like trees or topography. To enhance visibility on images the stick was marked with red tape on the end pointing north and dark objects were placed underneath both ends to create a colour contrast. The starting point of the drone was preferably selected at the top of a hill or at least halfway there, though this was not always possible. After take-off, the drone was elevated to 100 m above the starting point and positioned facing north. When the drone had to be started from the foot of a hill, it was elevated to 120 m, which is the manufacturer's maximum altitude by default. This was done to ensure a greater coverage of the area as well as a minimized risk of colliding with large trees at the top of the hill. After reaching the desired altitude, it was flown in a regular pattern over the fern

patch and the surrounding vegetation (Figure 7). This is also known as the lawnmower pattern. The drone's gimbal was positioned facing downwards in a - 90° angle. The drone was stopped in the air every few metres in order to take a picture. After every stop, the gimbal was readjusted to face downwards. Flying the drone in the lawnmower pattern in combination with taking pictures in a quick succession allows for a large overlap of images, which is desirable for merging these. Several factors lead to multiple visitations being needed for one plot. These were mainly due to weather conditions such as winds and rains decreasing the quality of images. Other times it was owed to malfunctioning of the drone or proximity to the airport that required unlocking specific areas for the drone to take off.

The ground sampled distance (GSD) was calculated as a function of maximum flight height over ground with the following formula (Propeller Aero 2021):

$$GSD_h = \frac{\text{Flight Height} \times \text{Sensor width}}{\text{Focal Length} \times \text{Image width}}$$

Given the flight height between 100 and 120 m, a sensor width of 5.842 cm, the focal length of 2.4 cm and the image width of 3000 pixels, the GSD lies between 8.11 and 9.74 cm. Since the drone only measures the distance to the ground from the starting point the resolution can change somewhat with topography. Therefore, the actual GSD

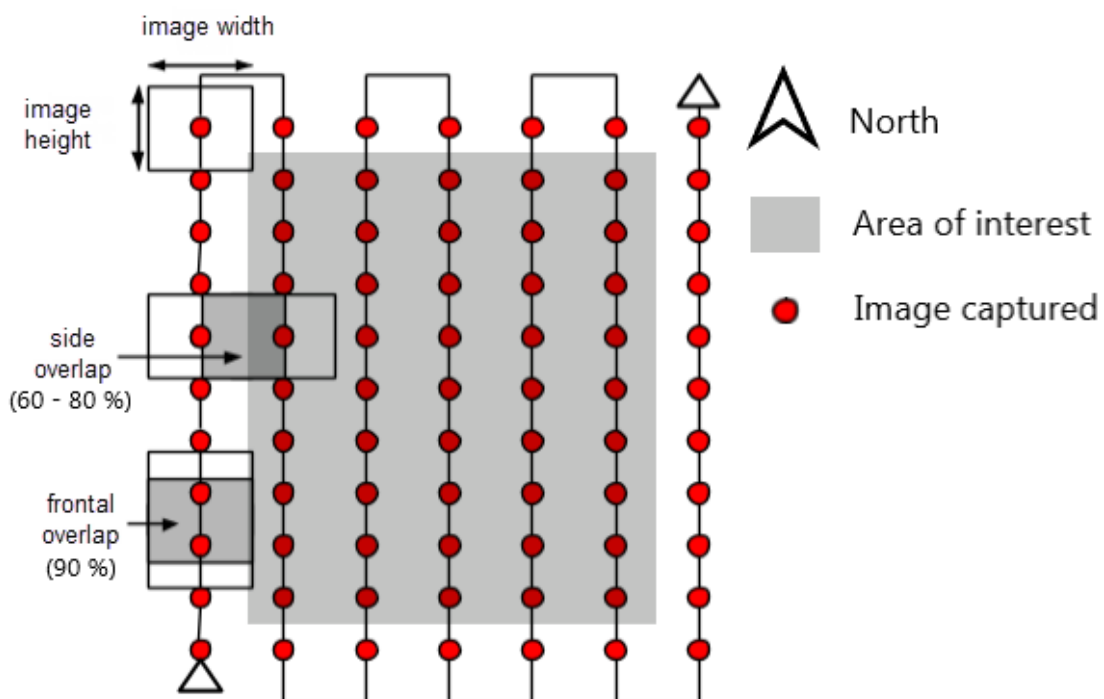


Figure 8: Schematic layout of drone flights in lawnmower pattern. The drone was positioned facing north taking images in a quick succession to get a desired frontal overlap of 90 % and side overlap of 60-80 %. Adapted from Aerotas (n.d.)

is lower, i.e. a higher value, for the majority of the image. In total, over 7,500 images were taken covering an area of approximately 404 ha.

2.4 Drone image processing

Drone images were uploaded in Agisoft Metashape 1.8.4 one plot at a time. Step by step - first dense point cloud, then mesh model followed by a digital elevation model (DEM) and finally orthomosaic – one large image in a GEOTIFF format was created for each plot. These images are georeferenced, meaning the location of each pixel with relation to the globe is known. However, given that the used drone is not designed for accurate mapping the georeferencing might be slightly inaccurate. Therefore, the images were imported in QGIS 3.1.6 and the ‘georeference’ tool used to improve their georeferencing accuracy. As this process did not work for every plot, since not all of them had markers to refer to, this procedure was omitted, and every image was used as it was to ensure comparability.

2.5 Area assessment of fern-dominated sites

The created GEOTIFFs were imported in QGIS 3.1.6 for area assessment of fern-dominated sites. For this a shapefile-layer with polygon geometry type was created. Then, for each of the plots, polygons were drawn around fern-dominated sites. When there was an obstruction in fern cover, for example through trees or erosion, an extra polygon was drawn around these. Using the formula ‘area (\$geometry)’ in the field calculator, the area of each polygon was calculated. The size of fern-dominated areas was added for each plot and from that the size of fern cover obstruction was deducted to receive the net area covered by ferns. In some instances, fern-dominated areas were detected that lied outside the area of interest (see Figure 8). For these cases the previously mentioned procedure was carried out if the beginning and the end of the fern patch was clearly visible and if the size of the patch was around 150 m² or larger. If either one of these prerequisites was not given, these patches were ignored.

2.6 Canopy cover

Unprocessed drone images were uploaded in ImageJ 1.53k and the 1.74 m reference stick used as scale. Areas were obtained by drawing a polygon around the crown of trees of which the DBH was measured. The crown diameters were calculated based on the crown area determined through these polygons. Given the tree species,



Figure 9: Screenshot of drone image in ImageJ. The crown circumference of a tree that was measured in the field and found again in the image is measured through drawing a line around the crown and using the reference stick for size rereference.

DBH and crown diameter, the idea was to create a correlation so the accumulated biomass could eventually be estimated from the crown area.

2.7 Satellite image acquisition and processing

In order to map the change in size of fern patches, the plan was to acquire the most recent satellite image as well as the oldest possible. Cloud cover should be as low as possible and SR high or very high. The drone images should function as a ground truthing of the latest satellite image. Sentinel-2 images from 2020 were first accessed through the Semi-Automatic Classification plugin (SCP) in QGIS. Additionally, a Sentinel-2 image from 2016 was accessed through the Google Earth Engine (GEE) plugin in QGIS. The area of fern cover was outlined as described above. However, it did not seem feasible to compare the results as the SR of Sentinel-2 images is 10 m at best, whereas the drone images have a SR of around 8 cm at best. Therefore, results using Sentinel-2 images were omitted. In search of higher resolution images, the GEE plugin in QGIS was used to obtain images in form of the Planet and NICFI Basemaps for Tropical Forest Monitoring (Planet 2023). However, since the basemap is a mosaic of images, it was quickly dismissed as it is not suited for the classification process that would be part of the evaluation (see further below). Two PlanetScope scenes, one captured on 3rd March 2022, the other one on 20th January 2017 were provided by Planet's Education and Research (E&R) Program (Planet Team 2022). This sensor has a SR of 3 m, is equipped with eight spectral bands and has a daily revisit time (ESA

2023a). Though, the scene of 2017 only has four available spectral bands. Additionally, one image of the European Space Agency's Pléiades constellation captured on 5th March 2015 was obtained. The sensor has a pansharpened SR of 0.5 m, four spectral bands and a repeat cycle of 26 days (ESA 2023b). Each scene was imported in QGIS and saved in a project file for further evaluation. The area of the plots was evaluated using the same procedure as described for the drone images. The PlanetScope scene of 2022 covered an area of 153 km², the one from 2017 132.5 km², and the Pléiades scene of 2015 covered an area of 158 km².

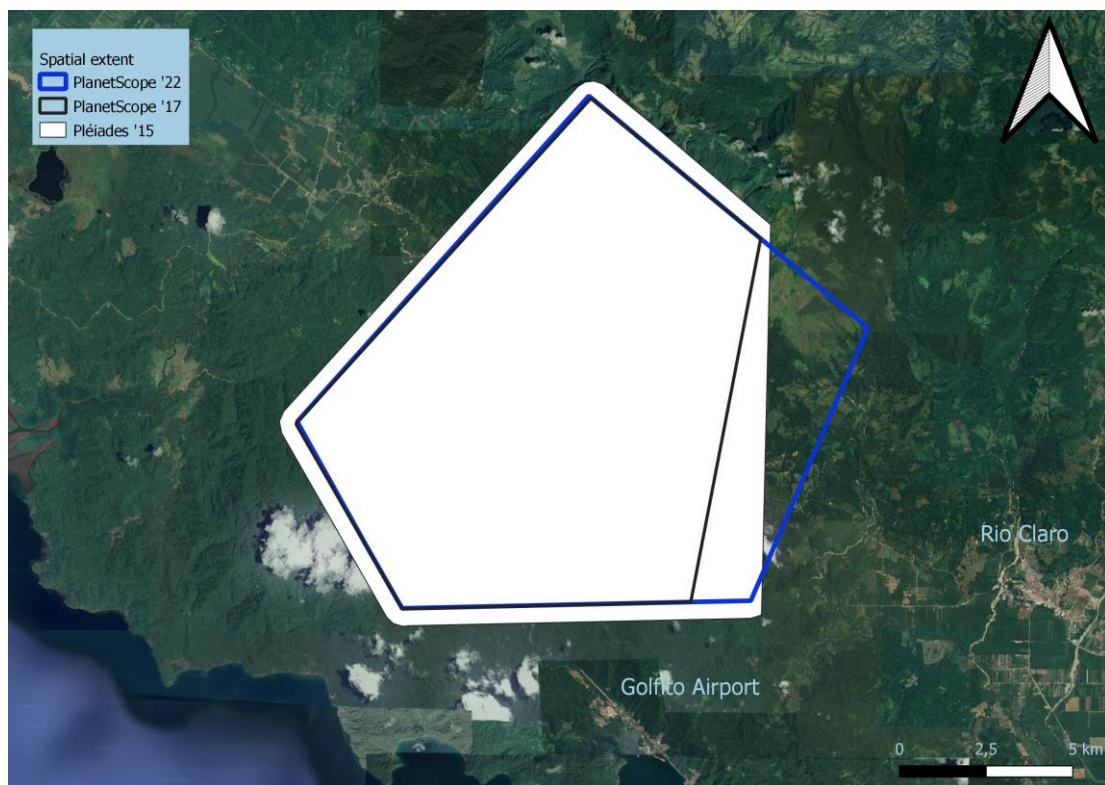


Figure 10: Comparison of the spatial extent of the different satellite scenes. The extent of the PlanetScope scene of 2022 is transparent and outlined in blue, the extent of the PlanetScope scene of 2017 is transparent and outlined in black and the extent of the Pléiades scene is depicted in white. Adapted from Google Earth (2015).

2.8 Aerial photograph evaluation

Aerial photographs taken in the vicinity of La Gamba in 1960, 1973, 1980, 1990, and 1998 were imported in QGIS. First, they were georeferenced using the 'georeference' tool. Then, they were checked for the visibility of ferns on the studied plots (see Figure 5). The images from 1960 to 1990 were black and white, therefore, no further processing was taken out with them. Additionally, a satellite image of 2007 was sighted in GoogleEarth to check for the visibility of ferns on the studied plots. For the image from 1998 the size of the fern-dominated area was evaluated for plots that were visible on the scenes. Only fern patches that existed and were measured in 2022 were taken into account so the change in the fern area could be mapped out.

2.9 Semi-automatic area assessment

For each PlanetScope and Pléiades scene a training input file was created using the SCP in QGIS. Within this file, regions of interest (ROIs) were created. A ROI is a polygon within a land cover type that holds information about its wavelength. Six main land cover types were detected and used as macro classes within the training files. These were: ‘Forest’, ‘Fern’, ‘Agriculture’ - which includes all agricultural land and meadows, ‘Settlement’ - which consists of houses and roads, ‘Water’ - which consists of rivers and riverbeds, and ‘Clouds’ - which consists of clouds and their shadows. The number of inputs for the training file for each sensor can be obtained from Table 1. For the PlanetScope scene of 2022, two separate training files with different ROIs were created to test the difference between a classification with more and less input. For the PlanetScope scene of 2017, training files with little input had outputs that were highly inaccurate. Additionally, the depicted area size of the scene was smaller than the prior one. Therefore, only one training file was used for this scene. The file size of the Pléiades scene of 2015 was multiple times larger than that of the other scenes. Hence, there was little experimentation with different numbers of inputs to keep lengthy processes to a minimum and only one training file was used. More input was added for ‘Forest’ as multiple forest patches were classified as ferns in a prior run. There were only three clouds on the scene which is why there was less input than in the other training files.

	<i>Pléiades</i> <i>'15</i>	<i>PlanetScope</i> <i>'17</i>	<i>PlanetScope '22</i> <i>(1st Classification)</i>	<i>PlanetScope '22</i> <i>(2nd Classification)</i>
<i>Forest</i>	15	12	5	12
<i>Fern</i>	14	14	10	14
<i>Agriculture</i>	14	13	8	13
<i>Settlement</i>	4	4	5	5
<i>Water</i>	5	5	5	5
<i>Clouds</i>	2	6	0	6
<i>Total</i>	<i>54</i>	<i>54</i>	<i>33</i>	<i>55</i>

Table 1: Number of inputs for each land cover class for each sensor and year.

The scenes were classified using the ‘Land Cover Signature Classification’ (LCS) and ‘Minimum Distance’ algorithm of the SCP. The following description of the classification is based on Congedo (2021). The LCS defines spectral thresholds for every ROI of the training input file. These thresholds define a spectral region for every land cover class. When running the classification, the spectral signature of each image pixel is compared to the spectral signature of the training input spectral signatures. This is

described by Fig. 11, where p_1 , p_2 , p_3 and p_4 depict pixels undergoing the classification process and g_a , g_b and g_c the land cover classes they are being compared to. If the spectral signature of a pixel is completely enclosed by the spectral region of one land cover class, it will be assigned to said land cover class. In Fig. 11, p_1 and p_2 are enclosed by the spectral regions of g_a and g_b and will therefore be assigned to the region enclosing them. p_3 cannot be assigned to a spectral signature by the LCS because it falls in the spectral region of both g_b and g_c . p_4 cannot be assigned to a spectral signature by the LCS because it does not fall in any spectral region of the hypothetical training file. Therefore, p_3 and p_4 are assigned to the closest spectral region according to the Minimum Distance algorithm.

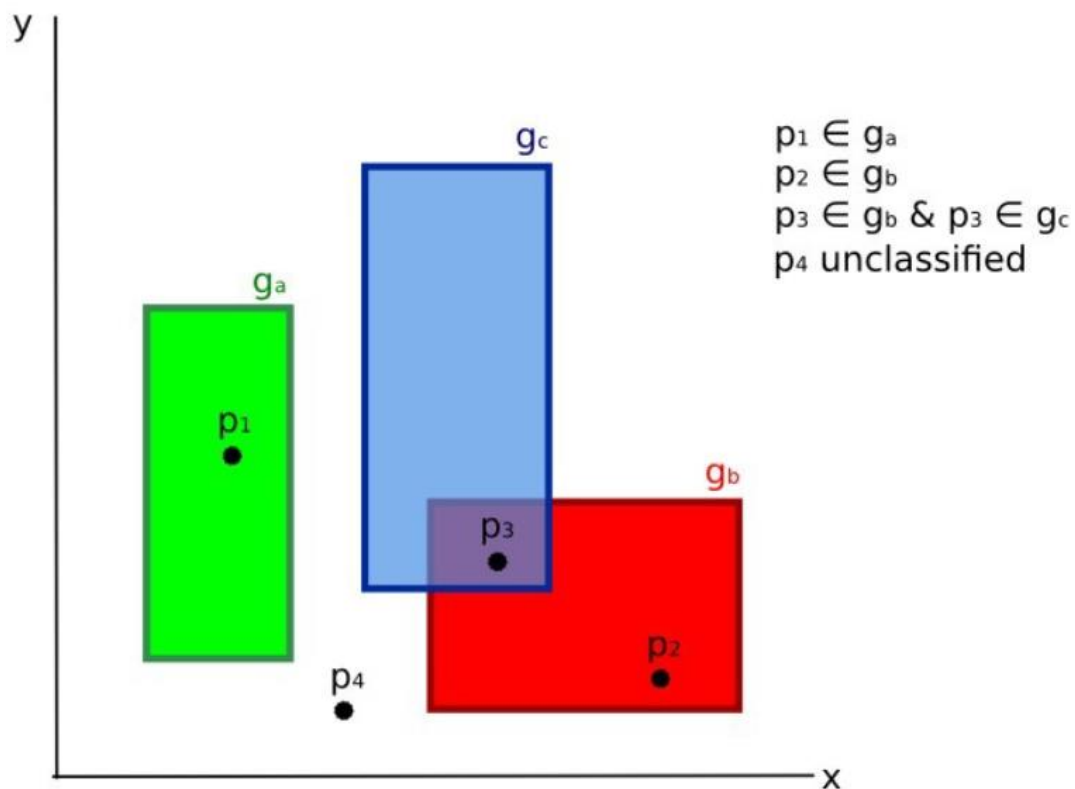


Figure 11: Visualisation of the Land Cover Signature Classification. The graph shows a hypothetical spectral range on the y and x axis. The spectral signature of pixels (p_1 , p_2 , p_3 and p_4) are compared to the spectral signature of land cover classes of a training input file (g_a , g_b , g_c and g_d). If the spectral signature of a pixel lies in the spectral region of one land cover class, the LCS will classify it as that land cover class (p_1 to g_a and p_2 as g_b). If the spectral signature of a pixel lies in the spectral region of more than one land cover class (p_3 in g_b and g_c) it cannot be classified by the LCS. p_4 cannot be classified by the LCS because it does not fall in any spectral region of the training input file. Source: Congedo (2021).

The classification resulted in a GEOTIFF of the scene that shows the classified areas in one of six colours corresponding to their land cover class i.e., a dark green for forests. This image was then converted into a vector layer. Afterwards, a new field with the formula 'area (\$geometry)' was added to the layer to calculate the area of the classified regions in the same way as in prior paragraphs. The calculated areas were

then assessed in two steps. First, the area within plot captured in the drone images was determined by using the 'identify features' tool. Fern areas, which belonged to one of the 23 plots were summed up to receive the total fern area per plot. Fern patches that were not assessed using the drone images were ignored unless they were connected to fern patches captured in the drone images. This way, no new patches are added so the actual area development of the plots could be evaluated. In the second step, the area of every pixel on the entire scene, that was classified as a fern, was assessed. For this, the attribute table was exported into an .csv file which was imported in R 3.6.1 for further assessment using the 'dplyr', 'tidyverse', and 'xlsx' packages. The results of the first step can be compared to the area assessment of the prior chapter to estimate the overall accuracy of the classification.

3. Results

3.1 Tree circumference measurements

In total, 137 tree circumferences were measured of which 126 were measured on plots that were flown over using the drone. 22 different tree species were identified, the species of five individuals could not be identified, mostly due to being smothered by climbing plants. The most frequently measured species was *Vochysia ferruginea* with 27 individuals. The lowest DBH (3.7 cm) measured was a *Luehea seemannii*, the largest DBH (82 cm) belonged to a *Vochysia ferruginea*. Only eight tree individuals whose stem diameters were measured could be identified on drone images with absolute certainty. The other 118 individuals were suspect to some level of uncertainty of which the identity of 26 individuals were purely speculative.

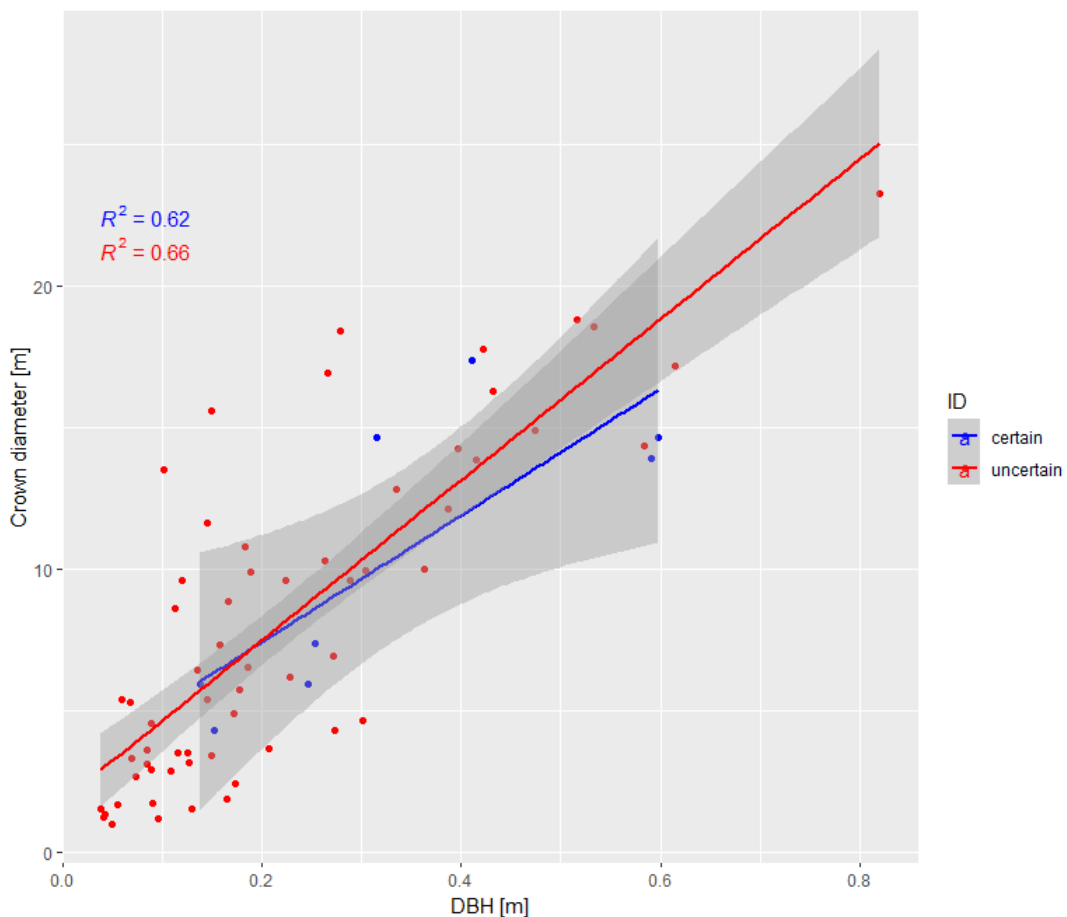


Figure 12: Relationship between crown diameter (y-axis) and diameter at breast height (x-axis). The blue points and line only include the eight individuals that could be linked with certainty, the red points and line show the 86 individuals that were linked with some uncertainty.

Therefore, the regression of the eight trees that were identified with certainty and the 86 trees with less certainty was compared. The correlation between DBH and crown diameter is rather linear and there is no difference between certain and uncertain individuals. Therefore, the potential error in identifying individuals does not matter for

this correlation. The DBH can be estimated from the crown diameter with an R^2 of 0.66 (Fig. 12).

3.3 Manual area assessment based on drone and Planet data from 2022

In the drone images, an area of 24 ha was dominated by *Dicranopteris pectinata*. This amounts to roughly 6 % of the total documented area of 404 ha. The rather small percentage can be explained by the square-shaped flight pattern. This becomes apparent in Fig. 13 a) where there is fern-dominated area in the centre and pasture in the east and west that cover roughly the same area. Fern-dominated area varied greatly as the smallest fern covered area was detected in plot 19 with a single fern patch of 266 m². In contrast, the largest fern covered area was detected in plot 13 with 38,900 m² divided in several patches (see Fig. 22). The mean fern-dominated area was 10,488.5 m², the median was 6,293 m².

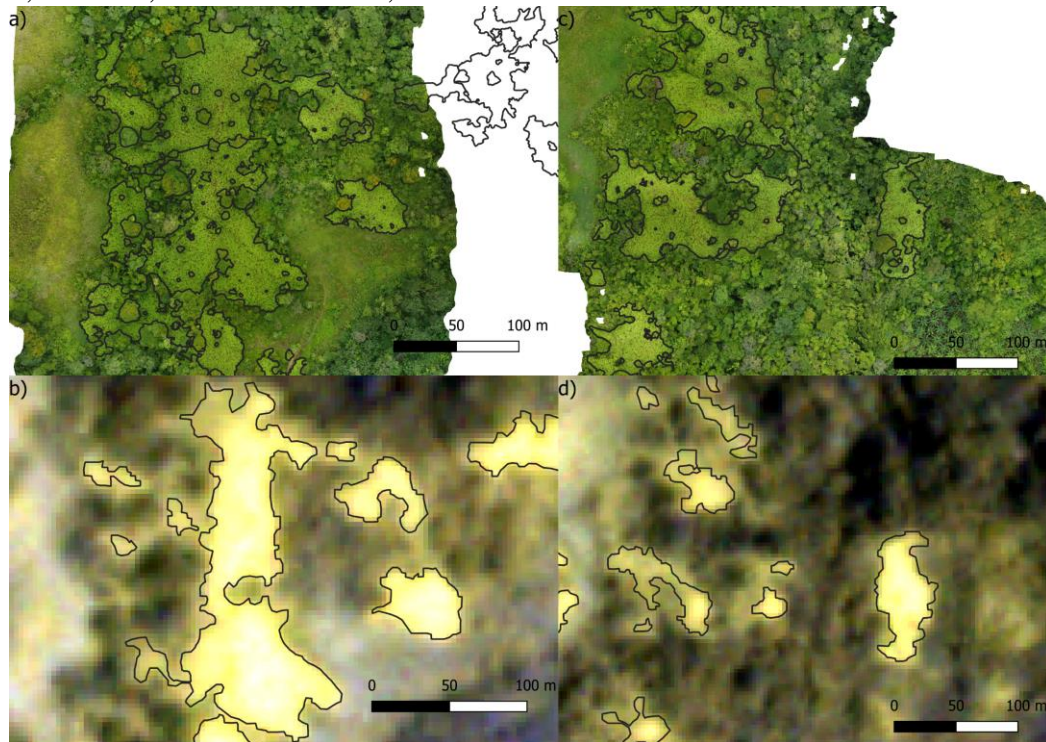


Figure 13: Comparison of drone images and PlanetScope scene of 2022. Part of plot 11 on drone image (a), part of plot 11 on PlanetScope scene (b). Part of plot 13 on drone image (c), and on PlanetScope scene (d).

The total fern area of the studied plots based on the PlanetScope scene of 2022 was 17.6 ha, which corresponds to 73 % of the area assessed using drone images. On average, fern-dominated area evaluated based on satellite images was 29 % smaller than in the drone images. Just as in the drone images, the smallest area was detected in plot 19 with 175 m² and the biggest area in plot 13 with 28,624 m² (see Fig. 22). The biggest relative difference comparing drone and satellite images occurred in plot 25.

Using the drone images, an area of 6,293 m² was evaluated compared to 2,414 m² in the satellite images which corresponds to 38 %. The biggest absolute difference occurred in plot 13 where 10,276 m² less fern-dominated area was detected relying on satellite images. The smallest absolute difference in size occurred in plot 19 with picking up 91 m² less with satellite images than drone images. In plot 24 the smallest relative difference was detected with satellite-based area assessment picking up 3 % more than the drone-based approach. Plot 8 was the only other plot where the fern area was larger in the satellite-based evaluation than in the drone-based one. The mean and median relative size difference of fern areas on studied plots was 71.4 and 71.7 %.

3.4 Semi-automatic classification of Planet data of 2022

The total fern area on studied plots determined by the first classification was 12.9 ha. For the second classification, it was 13 ha. This corresponds to around 73 and 74 % of the manually assessed area for the PlanetScope scene of 2022. Overall, less fern-dominated area was determined manually based on the satellite image than on the drone images. Both classifications mostly evaluated a smaller fern-dominated area

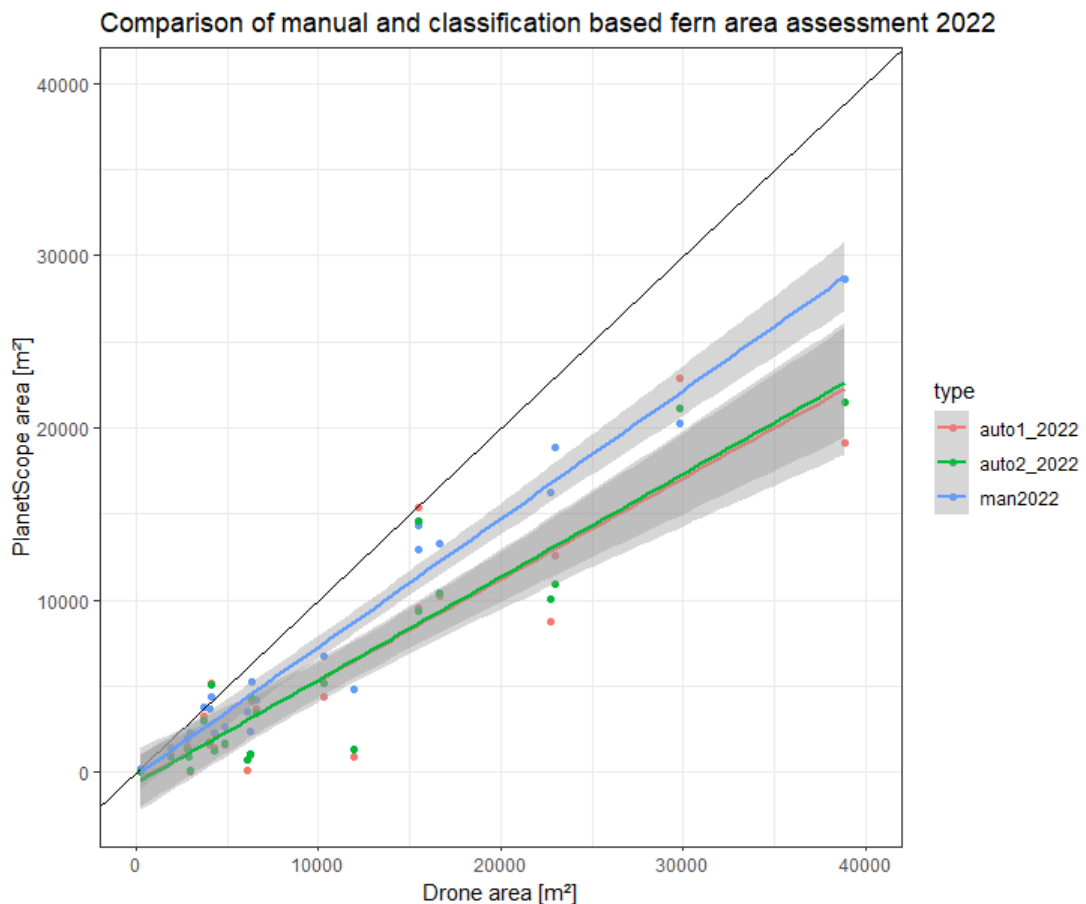


Figure 14: Comparison of the first classification (red), second classification (green) and manually assessed fern-dominated area (blue) of the PlanetScope scene of 2022.

than manually assessed with the satellite image (Fig. 14). However, on three plots the classifications determined larger areas. Both the first and the second classification did not pick up any fern-dominated area in plot 19. In plot 20, the first classification detected no *Dicranopteris*-dominated area, and the second classification marked only 144 m² as fern area, which is 6 % of the manually determined size. The largest absolute difference to the manual evaluation for the first classification occurred in plot 13 with 9,534 m² or 67 %. For the second classification, it arose in plot 21 with 7,953 m² or 58 %. Plot 12 is the plot with the largest relative accuracy for both (see Fig. 14 and Fig. 22). The first classification indicated 7 %, the second classification 2 % more area than manually assessed. The mean and median fern-dominated area of the first

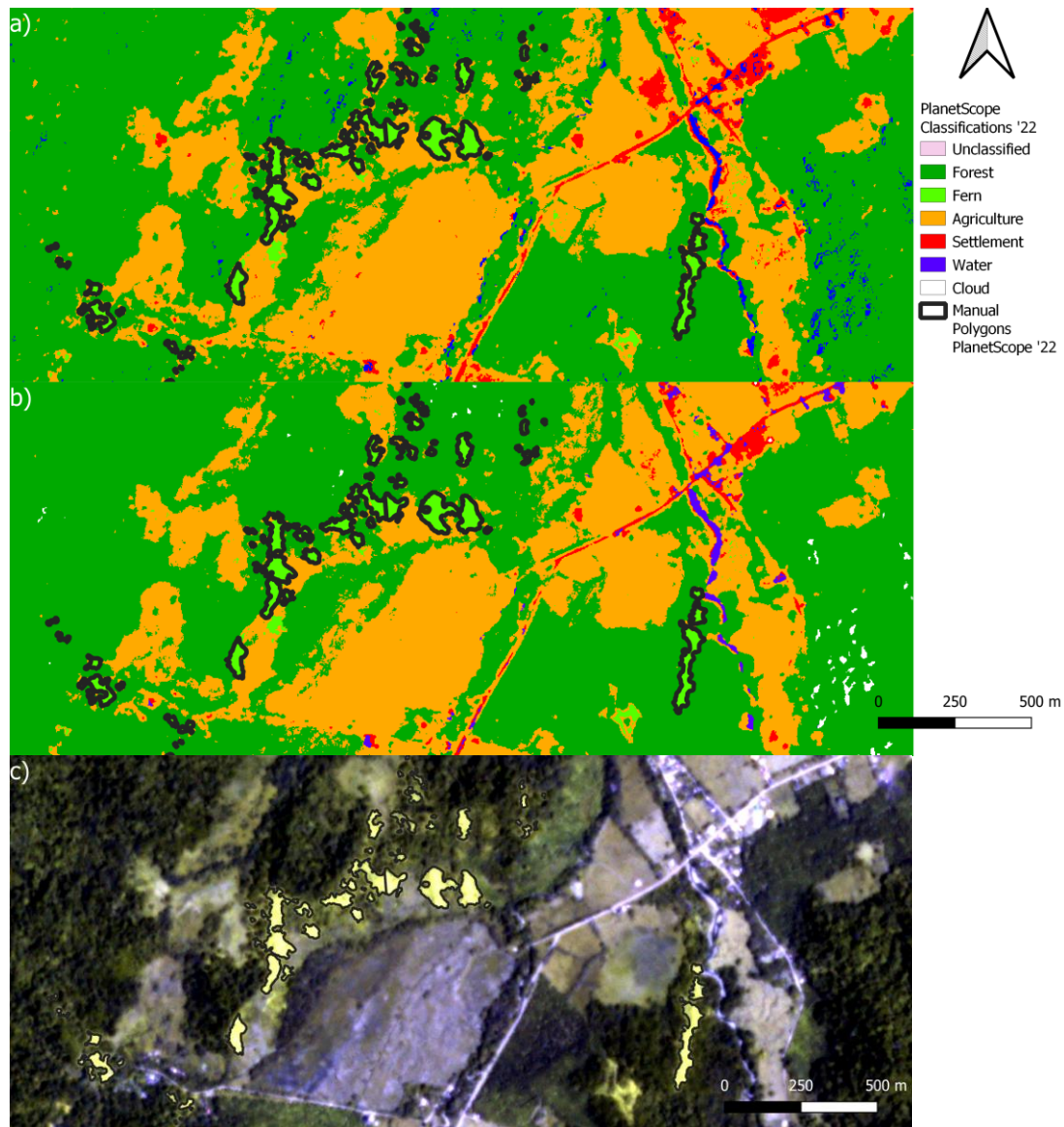


Figure 15: Comparison of clipped images of the classifications and the unclassified PlanetScope scene of 2022. a) first classification, b) second classification, and c) unclassified clip of the PlanetScope scene of 2022. The manually assessed fern-dominated areas are outlined in black.

classification are 62.5 and 66.7 % of the manually determined area. For the second classification, they are fairly similar with 63.3 and 67.3 %.

The total area of the PlanetScope scene of 2022 was 15,267.4 ha. In the first classification, 176.5 ha were classified as fern, which corresponds to 1.2 % of the whole area. If sites, where *Dicranopteris* cannot grow (clouds, settlement and water) are excluded, fern-dominated sites make up 1.3 % of the area, based on the first classification. In the second classification, 150.7 ha were classified as fern, which corresponds to roughly 1 %. If sites, where *Dicranopteris* cannot grow are excluded, fern-dominated sites make up 1.1 % of the area, based on the second classification. Fig. 15 shows that both classifications detected a similar fern-dominated area as manually assessed around the Tropical Field Station and that adding the class ‘Clouds’ led to different classification outputs.

3.5 Fern detection based on Planet data of 2017

The total fern-dominated area on studied plots was 9.3 ha. This corresponds to around 53 % of the satellite-based area of 2022. In plot 19 no *Dicranopteris* cover could be detected. Besides that, the smallest area was assessed in plot 20 with 304 m²

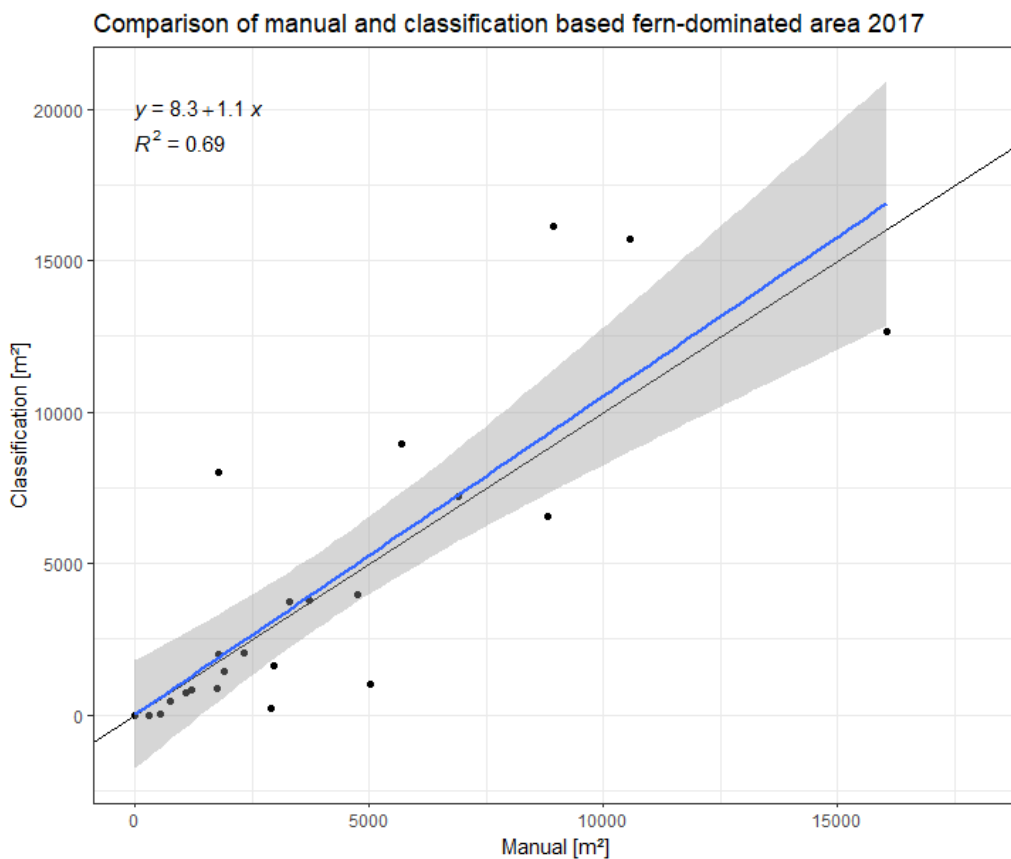


Figure 16: Area comparison between the manually assessed fern-dominated area (x-axis), and the area assessment based on the classification (y-axis) of the PlanetScope scene of 2017

dominated by ferns. The largest fern-dominated area was evaluated in plot 21 with 16,051 m². In comparison to 2022 all plots but two were smaller in size. The smallest relative and absolute difference in area occurred in plot 3 with 22 m² or 1 % less than in 2022. Excluding plot 19, the largest relative difference was detected in plot 20, which was 83 % smaller than in 2022. The biggest absolute difference was picked up in plot 13 with 18,065 m². Plot 1 was 519 m² or 12 % bigger than in 2022. The only other plot that was bigger than in 2022 was plot 6 with a difference of 392 m² or 29 %.

The total fern-dominated area on the plots according to the classification was 9.8 ha, which is 5 % more than manually assessed. On thirteen plots the classification determined areas smaller and on eight plots areas larger than manually assessed (Fig. 16). The R² of the correlation between manually and classified area based on the PlanetScope scene of 2017 was 0.69. The classification did not detect any *Dicranopteris* cover in plots 19 and 20, although there was visible fern cover in plot 20. The largest absolute difference to the manually assessed area was seen in plot 11, where fern cover was 7,220 m² larger in the classification (Fig. 22). In relative terms, the largest difference occurred in plot 8, where the semi-automatic classification produced an area 453 % larger than the manual assessment. Beside the two plots just mentioned, there

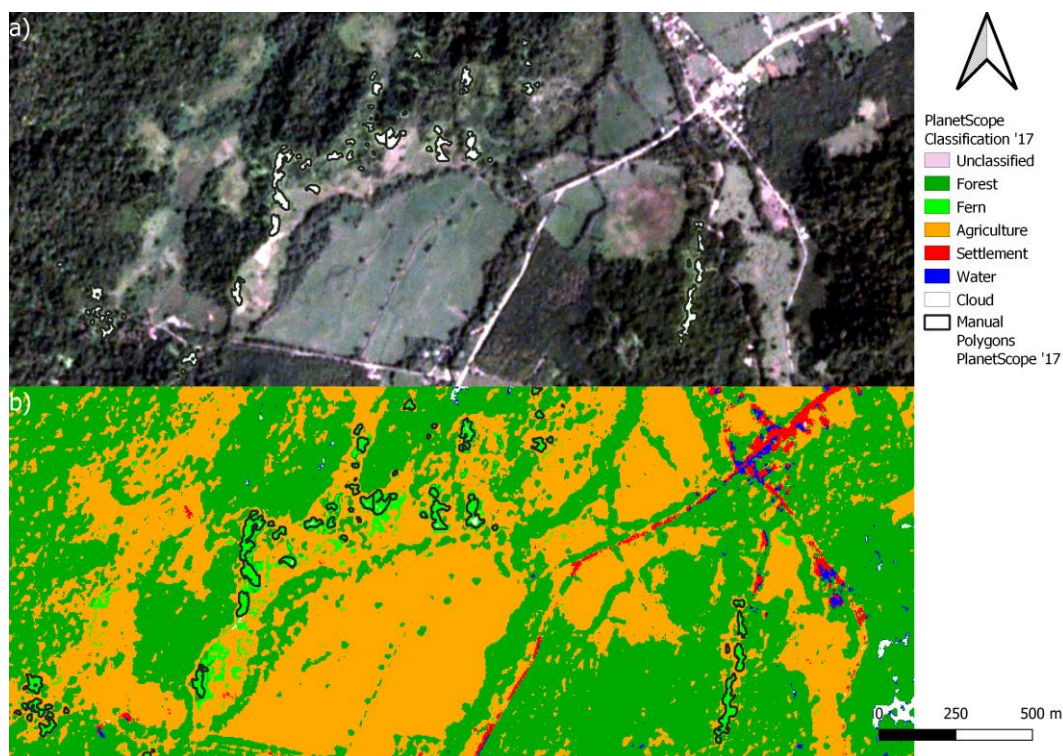


Figure 17: PlanetScope scene of 2017(a), and its classification (b). The manually assessed fern-dominated areas are outlined in black. In the bottom left corner are plots 1,2, and 3. Towards the centre and in the centre are plots 8, 11, 12, 13 and 23 (from left to right). In the bottom right corner is plot 10.

were six other plots where the classification assigned a larger area than in the manual approach.

The total area of the PlanetScope scene of 2017 was 13,151 ha. 66.1 ha were classified as fern, which corresponds to 0.5 % of the whole area. If sites, where *Dicranopteris* cannot grow (clouds, settlement and water) are being excluded, fern-dominated sites still only make up 0.5% of the area, based on the classification. Fig. 17 shows that the classification overestimates the fern-dominated area in some plots, such as in the middle of the figure while classifying other areas similar to the manual approach, such as in the bottom left and bottom right corner of the figure.

3.6 Fern detection based on Pléiades data of 2015

The total fern-dominated area picked up on studied plots was 16 ha which corresponds to around 91 % of the area assessed on the satellite image of 2022. As in 2017, no *Dicranopteris* cover could be detected in plot 19. It can therefore be assumed that this is a fairly new site. This is corroborated by a comparison with an image on GoogleEarth from February 2019, where it also appears to be closed forest. The only plot that was smaller than in 2017, was plot 16 with 336 m² less fern cover. The largest absolute difference in fern cover was detected in plot 13 with 9,573 m² (+ 91 %). The

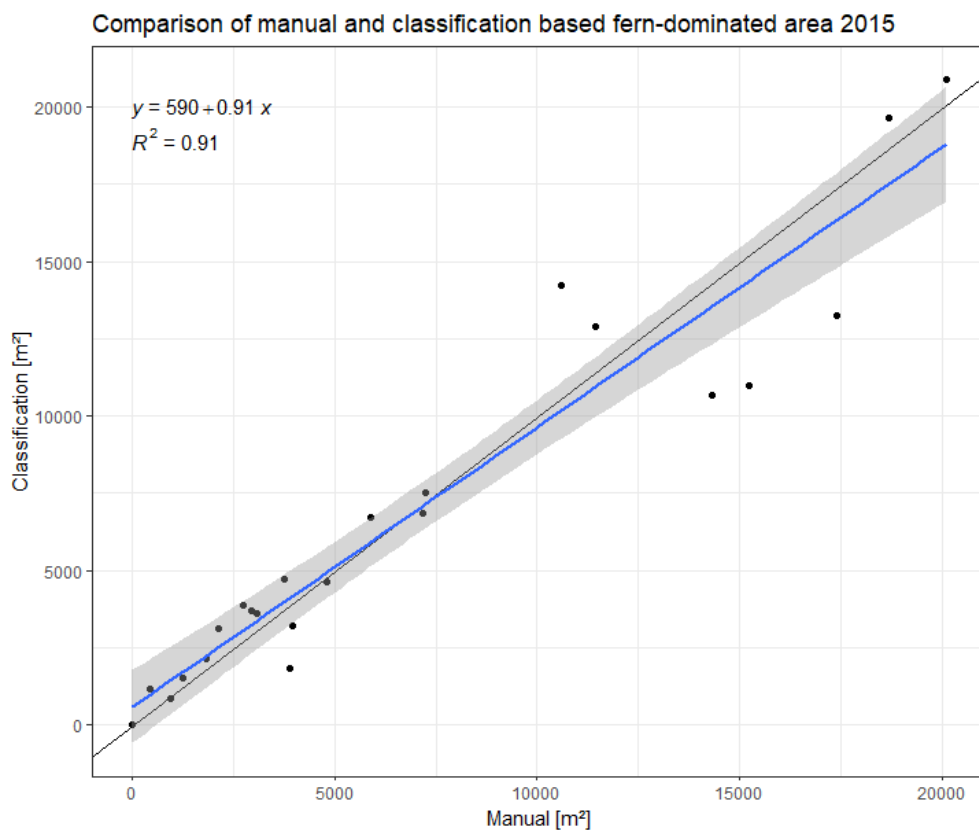


Figure 18: Area comparison between the manually assessed fern-dominated area (x-axis), and the area assessment based on the classification (y-axis) of the Pléiades scene of 2015

largest relative difference was seen in plot 15, where the fern cover was 7.5 times larger than in 2017.

When compared to the satellite-based assessment of 2022, twelve plots were smaller in 2015 and eleven were larger. The largest absolute difference was also detected in plot 13, which had an 8,492 m² smaller fern cover in 2015. The smallest relative and absolute difference occurred in plot 24, which was 45 m² smaller in 2015 which corresponds to a difference of 1 %. Given the difference in resolution, it seems more sensible to compare the Pléiades scene with the drone images. In that comparison, only two plots had a larger area in 2015. Plot 7 was 36 % bigger with 3,944 m² in contrast to 2,895 m². Plot 24 was only 61 m² or 2 % larger than in 2022. Plot 13 holds the largest absolute discrepancy with it being 18,768 m² smaller in 2015. In relative terms, plot 18 had the biggest difference. While the size in 2022 was 4,062 m² it was only 1,231 m² in 2015, which amounts to 30 %.

The total fern-dominated area on studied plots according to the classification was 15.8 ha which corresponds to 99 % of the area manually determined. On fourteen plots, the classification picked up a larger fern area than manually assessed (Fig. 18). Interestingly, the R² of 0.91 is a lot larger than that of the correlation of 2017. The correlation between manually and semi-automatically determined area of 2015 is strongly significant ($p = 1.38e^{-12}$). The largest relative discrepancy occurred in plot 16, where manually 411 m² of fern-dominated area were evaluated and through classification 1,174 m² were identified as fern-dominated. This is an increase of 186 %. The largest absolute difference can be seen in plot 11, where the classification determined 10,964 m². This is 4,278 m² less than manually assessed. The smallest relative discrepancy occurred in plot 2, where an area of 4,641 m² was classified. This is 167 m² or 3 % less than in the manual evaluation. In absolute terms, the smallest difference can be seen in plot 20, where the classification amounted to 870 m², which is 63 m² less than manually determined.

The total area of the Pléiades scene of 2015 was 15791.5 ha. 1,714 ha were classified as fern, which corresponds to 11 % of the total area. If only sites, where *Dicranopteris* can grow are being looked at, still 11 % of the area are comprised of fern-dominated area according to the classification of the Pléiades scene of 2015. Fig.19 shows that the classification determines fern-dominated areas in plots well but overestimates the overall area by falsely classifying patches in forests and palm plantations.

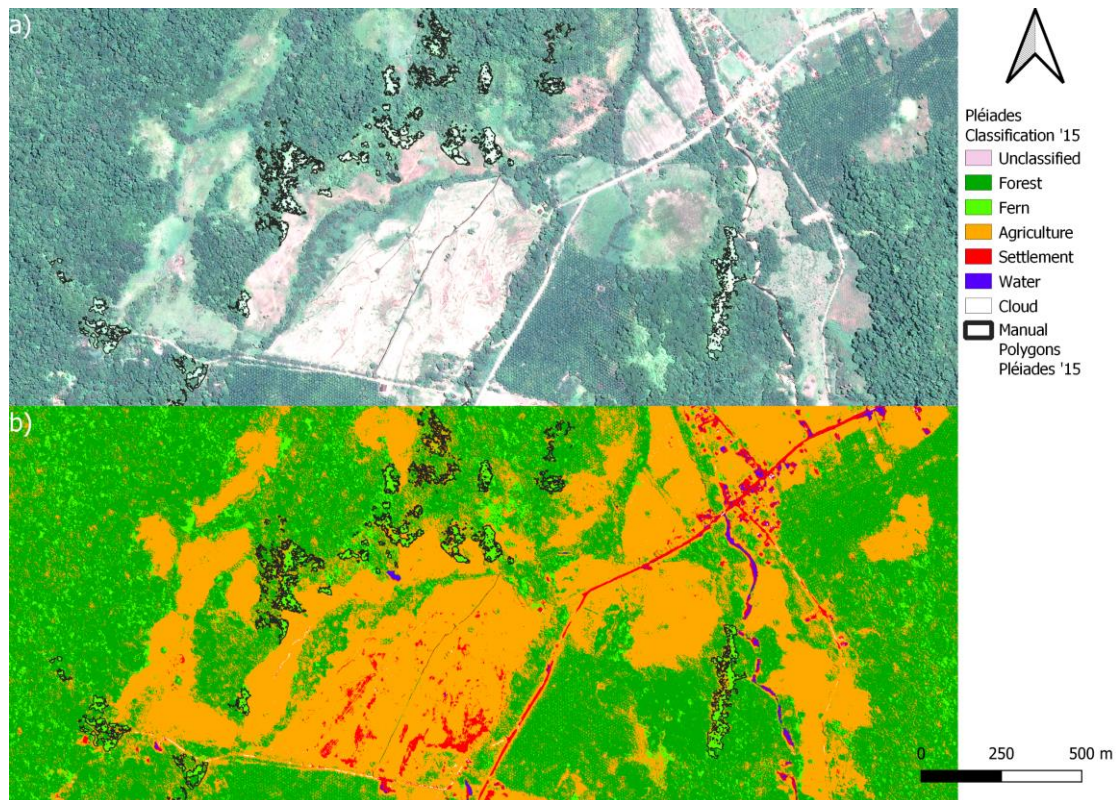


Figure 19: Comparison of the Pléiades scene of 2015 a), and the classification of the Pléiades scene of 2015 b). The manually assessed fern-dominated areas are outlined in black. In the bottom left corner are plots 1,2, and 3. Towards the centre and in the centre are plots 8, 11, 12, 13 and 23 (from left to right). In the bottom right corner is plot 10.

3.7 Evaluation of aerial photography of different time steps

Not all plots were visible in the aerial photography (see Table 2). In the image of 1960, there is a potential *Dicranopteris* cover on several studied plots, however the quality of the image did not allow for a precise distinction between fern-dominated sites and other open sites, such as agricultural land. The quality of the image of 1973 was better than that of 1960, and showed *Dicranopteris* cover in plots 7, 9, and 25. Plots 7 and 9 were clearly covered in fern on the image of 1980, however for plot 25 this could not be confirmed. The image of 1990 did not allow for an accurate distinction of fern-dominated sites and other open landscapes. As such, only on plot 25 could a *Dicranopteris* cover be confirmed. The only sites that were visible in the images of 1998 were plots 14, 15, 19, 20 and 21, but plots 15, 19, and 20 had no visible fern cover. Plot 14 had an area of 2,788 m², which is 88 % smaller than on the drone images of 2022. The fern-dominated area in plot 21 was 8,420 m² which is 37 % of the cover in 2022. The total fern-dominated area determined on the photograph of 1998 was 1.1 ha.

	1960	1973	1980	1990	1998	2007
Plot 1						x
Plot 2						x
Plot 3						x
Plot 4						x
Plot 5						
Plot 6						x
Plot 7		x	x			x
Plot 8						x
Plot 9		x	x			x
Plot 10	?					x
Plot 11						x
Plot 12	?	?				x
Plot 13	?	?				x
Plot 14					x	x
Plot 15						x
Plot 16						?
Plot 17			?			x
Plot 18						x
Plot 19						
Plot 20	?					x
Plot 21					x	x
Plot 22						x
Plot 23						x
Plot 24						x
Plot 25		x	?	x		x

Table 2: Presence of *Dicranopteris* cover on studied plots for aerial photography and Google Earth image of different years. Cells marked in dark green are visible on the image but have no visible fern cover. For grey cells that are marked with a "?", *Dicranopteris* cannot be confirmed with absolute certainty. Light-green cells marked with a "x" contain fern-dominated area.

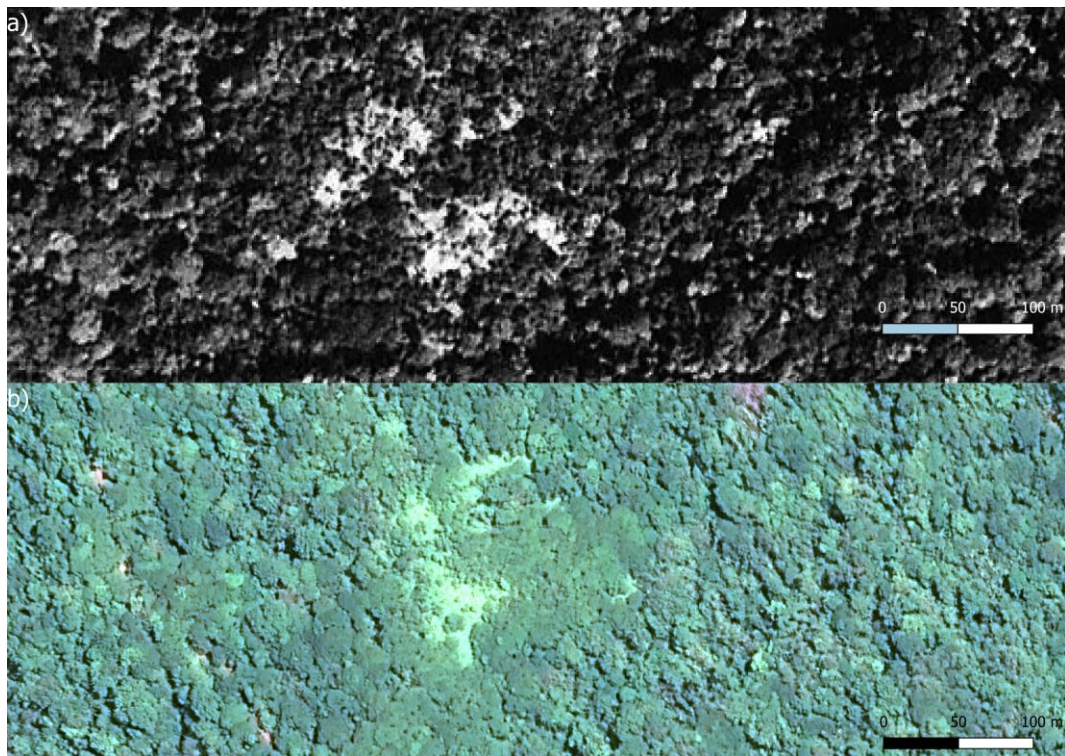


Figure 20: Plot 25 in a) 1973 and b) 2015. Note: Scale might not be accurate. Pléiades image was used for having the best visibility of this site.

3.8 Comparison of assessed area

Comparing the total area that was manually assessed for each year and sensor, the largest fern-dominated area was picked up using the drone in 2022 and the smallest by the orthoimage of 1998 (Fig. 21), but only five of the 23 plots were visible on the latter. The same relation can be seen if the plots are compared individually (Fig. 22).

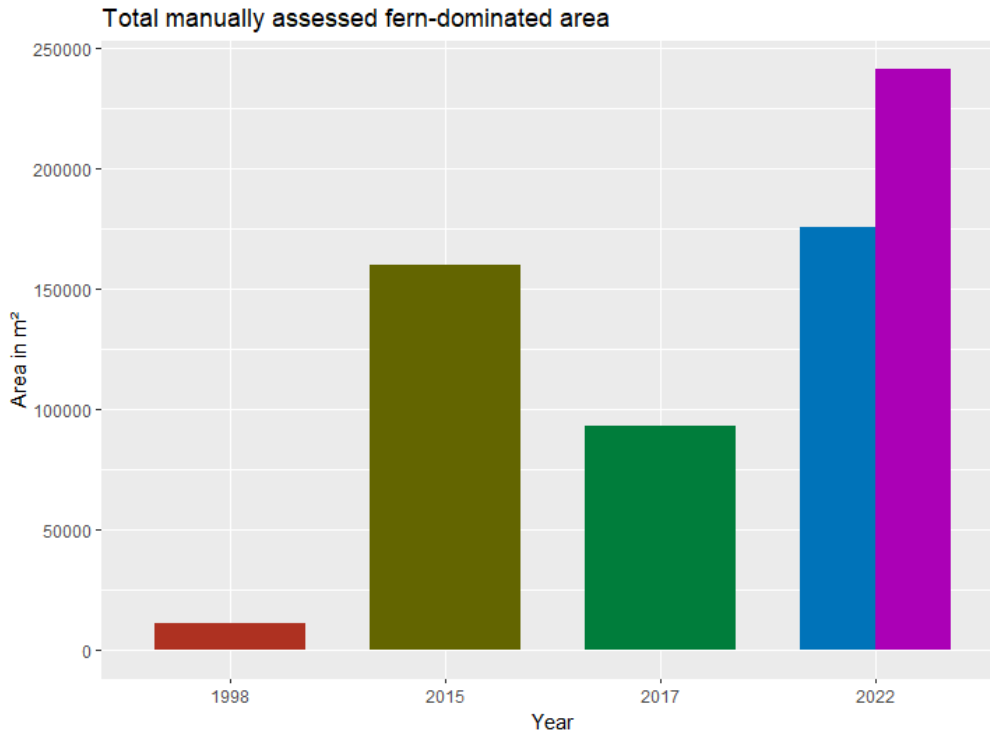


Figure 21: Total manually assessed fern-dominated area per year in m². The red bar shows the area determined on the aerial photography of 1998. The brown bar depicts the evaluated area based on the Pléiades scene of 2015. The green bar shows the area determined with the PlanetScope scene of 2017. The blue bar is based on the PlanetScope scene, and the purple bar based on the drone images of 2022.

However, for the other sensors the individual size comparison is not as straightforward. The second highest total fern-dominated area was evaluated using the PlanetScope scene of 2022. However, in eleven plots the area determined through the Pléiades scene of 2015 was larger. Whether plots were located next to forests or agricultural land had no influence on the area development as all but one plot were larger in the PlanetScope scene of 2017 than in the PlanetScope scene of 2022. The same was the case when comparing areas of the Pléiades scene of 2015 with the drone images of 2022.

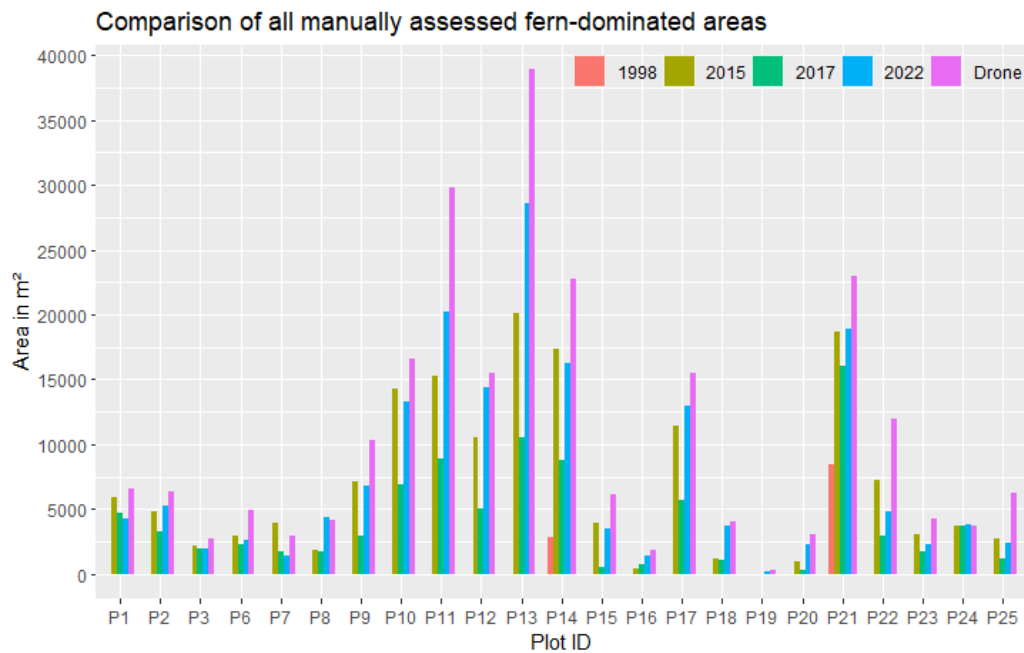


Figure 22: Plotwise comparison between the fern-covered area assessed based on the aerial photography of 1998 (red), Pléiades scene of 2015 (brown), PlanetScope scene of 2017 (green), PlanetScope scene of 2022 (blue), and drone imagery of 2022 (purple). Note: P4 and P5 are the ones that could not be sampled.

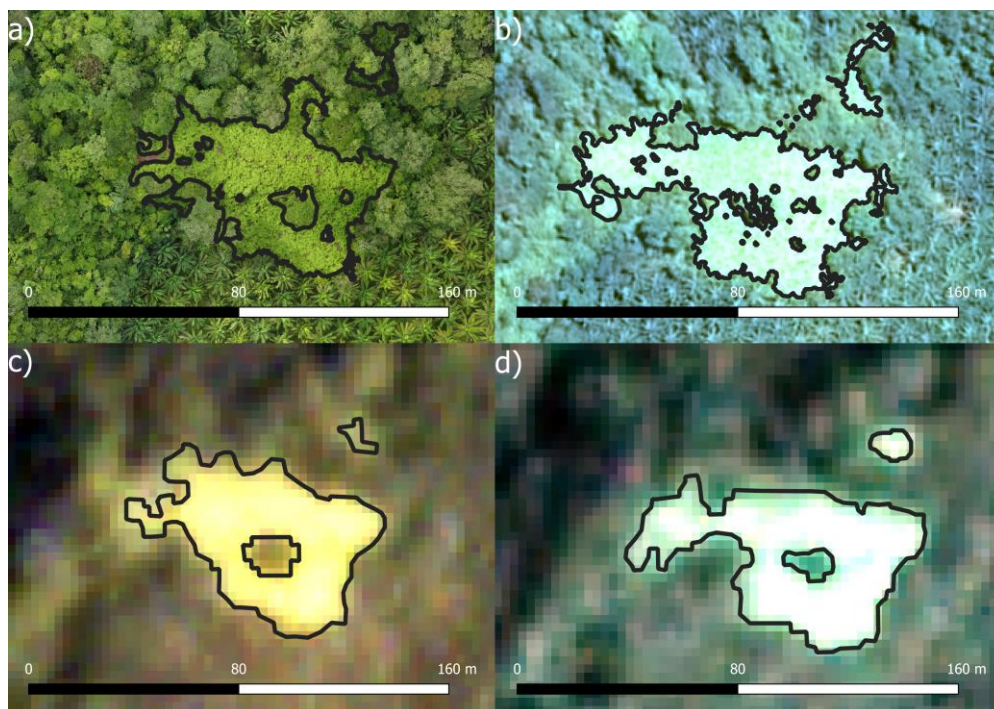


Figure 23: Comparison of Plot 24 for different sensors and time. a) Drone imagery of 2022, b) Pléiades scene of 2015, c) PlanetScope scene of 2022 and d) PlanetScope scene of 2017. Outlined in black are the drawn polygons for area assessment of ferns and trees.

Figure 23 shows a comparison between different sensors and years for plot 24, which resulted in similar cover estimates. The smallest area was determined using the drone with 3,682 m², the largest was picked up with the on the PlanetScope scene of 2022 with 3,788 m². It becomes evident, that with coarser resolution small trees within the thicket are not visible. In contrast, figure 24 shows plot 14, which had varying fern-

dominated areas. The large patch in the south-western corner does not seem to have existed in 1998. Plot 14 is surrounded by both agricultural and forested land and fern-dominated areas increased in both.

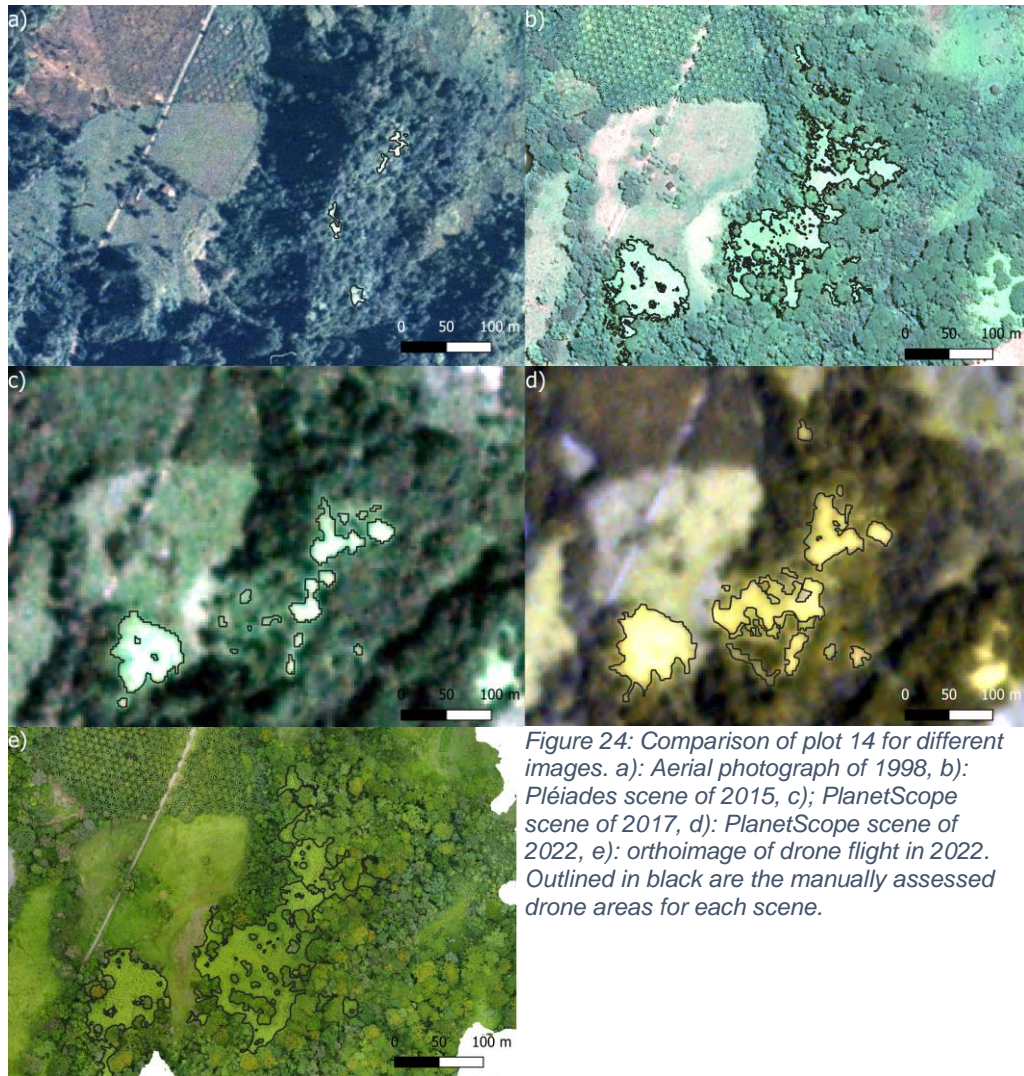


Figure 24: Comparison of plot 14 for different images. a): Aerial photograph of 1998, b): Pléiades scene of 2015, c): PlanetScope scene of 2017, d): PlanetScope scene of 2022, e): orthoimage of drone flight in 2022. Outlined in black are the manually assessed drone areas for each scene.

The composition of classified land cover classes varied between the classifications. All classifications had similar outputs for agriculture and settlement. The PlanetScope classifications had similar outputs for ferns and forests, however the classification for the Pléiades scene of 2015 had a smaller output in forests but a markedly larger output in ferns. Adding clouds as an additional class to the second classification of the PlanetScope scene of 2022 resulted in mostly areas classified as water being classified as clouds.

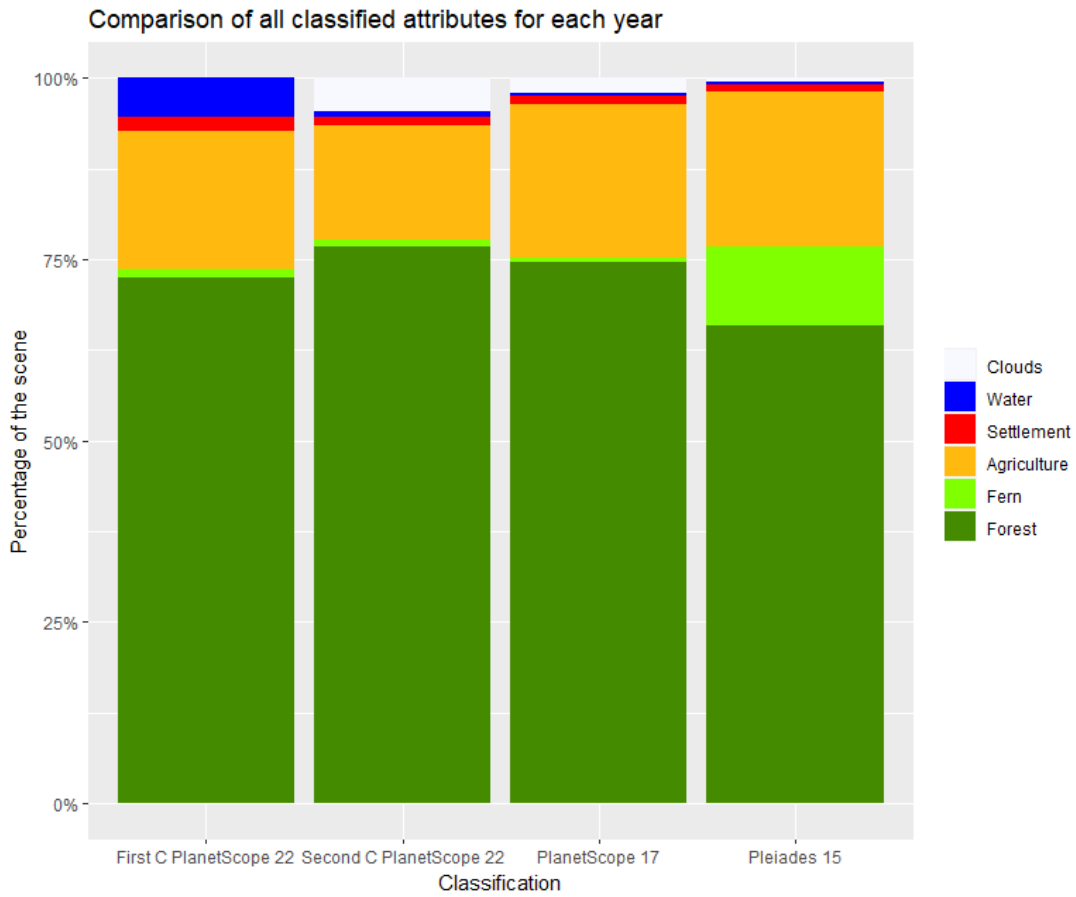


Figure 25: Comparison of the composition of land cover classes for all for each year. From left to right: First PlanetScope classification of 2022, second PlanetScope classification of 2022, PlanetScope classification of 2017, and Pléiades classification of 2015. Land cover classes from top to bottom: Clouds, water, settlement, agriculture, fern, and forest.

4. Discussion

4.1 Correlating DBH and crown area

It would have been interesting to have a sufficient number of trees whose DBH and crown area were matched. Ideally, a coefficient or formula could be derived from this correlation, in which the crown area could be inserted, that results in an estimation of the tree's biomass. The crown area could be derived from classifications in the same way plots' fern areas were derived from the classifications. Unfortunately measuring the DBH was no simple task in *Dicranopteris* thickets as it required slashing a path towards the trees using a machete. As MacCaughey (1918) points out, this is strenuous and leads to frequent tripping as well as wounding on the sharp edges left behind by the cut fern. Injuries not only occur by tripping over the fern itself. The thickets have a fairly homogenous canopy cover which makes projecting the topography underneath this cover difficult. Sudden drops of several meters are not rare. Therefore, only 92 trees could be sampled in the first place. Surprisingly, finding the measured trees on the images was not easy either, despite taking meticulous notes to aid identification. For instance, Plot 10 was the only site that contained a palm. Therefore, this prominent palm and the surrounding three *Vochysia ferruginea* individuals were measured with a detailed description of their location in relation to the palm. On the drone images, the palm tree could not be detected and near the location where it was assumed to be, the crown of what seemed to be only one *Vochysia ferruginea* individual was visible. Only eight trees could be identified on drone images with certainty. However, the correlation between DBH and crown area for these trees did not differ from the other 86 trees identified with some uncertainties. The R^2 of the correlation DBH ~ crown area was 0.66. If DBH is used to estimate biomass, the accuracy for biomass estimates therefore is only 66 %. In addition, wood density would be needed to calculate biomass, and this requires identifying the tree species, which is hardly possible from aerial images.

4.2 Drone campaign

Some of the aspects of the drone campaign and its results could have been optimised. For instance, the flight patterns could have been set automatically, which might have resulted in a larger overlap of more pictures, which in turn leads to more pictures being aligned and thus, a better overall quality of the orthoimages (Eisenbeiss and Sauerbier 2019). Additionally, calibrating the camera and setting the reference stick as scale would have improved the precision of the images. Ground control points and RTK (Real Time Kinematic) positioning are usually used in drone campaigns to increase the accuracy of the digital surface model and georeferencing (Forlani et al. 2018). Lastly, the used drone is not designed for mapping. As such, it does not contain software for automating flight patterns or have a RTK module as opposed to other models of the manufacturer. Most of these shortcomings stem from a limited knowledge in remote sensing and a short timeframe in which several, more basic preparations such as acquiring and registering the drone had to be taken out. These are also the main reasons why many of the methods were derived through trial and error. For instance, the idea of image processing in Agisoft Metashape instead of using the raw images was only adopted after the second flight was carried out. More time for preparation could have helped overcoming some of these issues, though this would have also meant investing a considerably larger amount of time than designated for these.

Although, happening largely inadvertently, the shortcomings can simulate accurate conditions for the aim of finding out, if the methods can be used by landowners as opposed to remote sensing experts. The used drone is comparatively cheap and easy to use. Thus, it is appropriate for ground truthing, especially in harsh terrains. In this study, it helped to identify fern patches even if they do not reflect in the characteristic green (see Fig. 23). However, in several cases fern patches seemed larger on the ground than on the images, when they are partly covered by tree crowns. Since this is a general issue of a view from above, it also applies for aerial and satellite imagery.

4.3 Fern-dominated area assessment

The number of polygons drawn to assess fern-dominated area and its obstructions varied between the different sensors. For the PlanetScope scenes of 2022 and 2017 155 and 160 polygons were drawn, respectively, for the drone imagery 794 and for the Pléiades scene 3062. This was because sensors with a higher SR enable a more detailed evaluation. As SR indicates the smallest object that can be picked up by a sensor (Liang 2012), it is not very surprising as seen in Fig. 23. Only a larger tree is circled as an obstruction in the PlanetScope images, while the drone and Pléiades images depict several smaller trees, too. The drone images were captured just weeks after the PlanetScope image of 2022. Yet, if the drone images had not been taken, several fern-dominated patches would not have been detected, due to lacking the characteristic reflection (as described above). Especially patches surrounded by forests were not always easily detected, even if they were visible in the drone images. To the viewer, they often seem like a forest patch that looks slightly different, e.g. due to hosting different species, or they are not all distinguishable from other forests. This could explain the large area discrepancy between the PlanetScope scene of 2017, where no ground truthing took place, and the other images. On the other hand, several areas look similar to *Dicranopteris* cover but are in fact covered by other plants. On the studied plots those were mostly covered by lianas (*Davilla sp.*). This observation is supported by Takeshige et al. (2022), whose classification accuracy improved when *Dicranopteris linearis* and vines were grouped as one.

Adding more inputs to the classification of the PlanetScope scene of 2022 did not affect the classified fern-dominated areas much. However, this was only tested with one differing file that already had a considerable number of inputs in ferns, which was the only variable the accuracy was tested for. Fern-dominated land was detected in plot 20 of the second classification, albeit 6 % of the manually assessed area. The first classification did not identify any fern cover on this plot and therefore seems less favourable. Upon inspection of Fig. 15, it is noticeable that some spots in the east of the images were classified as water in the first classification and as clouds in the second classification. While it is not correct that these spots are clouds, the classification is not incorrect as the class 'Clouds' also consists of shadows. Therefore, it can be assumed that the accuracy across classes did improve. Overall, it shows that the

quality of the inputs and appropriate land cover class selection is more important than mere quantity of inputs.

The difference in classification outputs between both PlanetScope scenes and the Pléiades scene of 2015 highlights this as well (Fig. 25). The file size of the Pléiades scene was many times larger than that of the other scenes, which resulted in very slow processing. As a consequence, the testing of classification settings had to be reduced to safe time. This in turn may have resulted in a low overall accuracy of the classification. The used classification is pixel-based, i.e. it only refers to the spectral information of each pixel in the image (Heinrich et al. 2009). On the other hand, object-based classifications group adjacent pixels and classify the resulting polygon of pixels (Jensen JR. et al. 2008). Object-based classifications have shown to outperform other classification methods (Weih and Riggan 2010). Therefore, using an object-based classification, potentially 'Random Forest', could have led to better results.

4.4 *Dicranopteris* development

The hypothesis, that *Dicranopteris* cover recedes in the presence of trees cannot be confirmed nor denied generally. In some patches, trees seem to regain dominance, while the fern-dominated area expands in other patches where trees were present. This could mean that *Dicranopteris* can outcompete trees at least on some sites, or that disturbance increases the open area, which is then taken over by ferns rather than regenerating trees. The hypothesis, that *Dicranopteris* cover expands in the absence of trees cannot be generally confirmed either. On several sites, especially around plots 8, 11, 12, and 13 fern cover increases onto the adjacent pastures. In some cases, this happens without relying on vegetative spread as the patches were not always connected. However, on other sites, such as plots 14 and 15, this development is not as apparent with fern cover barely expanding onto the adjacent pasture in the past seven years. One explanation could be the flat nature of the pasture on plots 14 and 15 as opposed to the more uneven, sometimes sloped pasture in the area of plots 8 and 11 to 13. Therefore, the risk of a *Dicranopteris* expansion could be higher in sloped sites than in plain sites possibly due to a competitive advantage. Walker et al. (2013) showed that slope had a strong positive influence on the abundance of *Dicranopteris pectinata*, which corroborates this. Another explanation could come from the cattle favouring flat areas and therefore either mechanically damaging the ferns or compacting the soils so that it cannot root there. Perhaps this could also be attributed to the

age of the sites. There seems to have been a lot of development around plots 8, 11, 12, and 13 in recent years (see Fig. 15, 17 and 19). At the same time, land-use around plots 14 and 15 did not change much since 1998 (see Fig. 24). Disturbance through land-use change could result in clearings, in which *Dicranopteris* and other organisms can invade. *Dicranopteris* may be particularly competitive on acidic and nutrient-poor soils (Zhao et al. 2012), and soils on pastures tend to be more nutrient rich.

If all manually assessed fern-dominated areas are being looked at, the overall size has increased over the years. Furthermore, the hypothesis that there will be more sites dominated by *Dicranopteris* was supported for the studied plots as five plots with fern cover in 2022 were visible on the aerial image of 1998, of which only two had a visible fern cover. This means the other three sites only established after these images were captured. According to the classification of the Pléiades scene of 2015, which on average classified an area 9 % larger than manually assessed as fern, the fern-dominated area on the scene of 2015 is 11 % of the total area. In contrast, both classifications of the PlanetScope scene of 2022 classified an area on average 33 % lower than manually determined. Both classify an area of around 1% of the total area as fern. Given the differing classification outputs, a comparison of the classification of the Pléiades scene with the others does not seem feasible. In the classification of 2017, which underestimated fern-dominated area by 25 % on average, *Dicranopteris* cover was classified on 0.5 % of the whole scene. Comparing the fern-dominated area based on the PlanetScope scenes of 2017 and 2022 may also support the hypothesis that more sites will be dominated by *Dicranopteris* with time. The manually determined fern cover in 2022 was smaller when based on satellite images than in the drone-based approach. This seems to stem from the coarser SR of the PlanetScope sensor. If this observation is extrapolated, it can be assumed that the lower the spatial resolution, the lower the assessed fern-dominated area. This in turn would mean that the actual area with *Dicranopteris* cover is even higher.

Although the shape of the fern thicket on plot 25 has changed between 1973 and 2022, the comparison shows that once established, *Dicranopteris pectinata* can be persistent for at least 49 years in the vicinity of La Gamba. Given the little development of the site, it is clear that succession is arrested. The strong persistence and its implications for forest regeneration highlight the questionable nature of distinguishing persistent

states merely by occurring for more or less than 100 years, as suggested by Thrippleton et al. (2018).

4.5 Biomass accumulation

Wyns (2015) calculated the aboveground biomass of *D. pectinata* thickets in the vicinity of the Tropical Field Station of La Gamba. On average, the ferns accumulated $60,8 \pm 5,0$ Mg/ha of biomass. If multiplied by the areas evaluated on the studied plots, it would amount to around 973 Mg in 2015 and 1,064 Mg or 1,459 Mg in 2022 depending on underlying the satellite-based or drone-based approach for the calculation. Using the same calculation with the results of the second classification of the PlanetScope scene of 2022, around 9,163 Mg would be accumulated by *D. pectinata* in the vicinity of the Tropical Field Station of La Gamba.

Oberleitner et al. (2021) calculated around 164 Mg/ha biomass accumulation after 20 years of secondary forest succession. The same calculation as above would result in 2,624 Mg in 2015 and 2,870 Mg or 3,936 Mg that could have been accumulated on the studied plots if good functioning forests grew there. Based on the second classification of the PlanetScope scene of 2022, around 24,715 Mg could have been accumulated by forests. This shows that delayed forest regeneration by *Dicranopteris* also reduces carbon sequestration and the related ecosystem services (FAO 2002b). Furthermore, this supports the notion of Ghazoul et al. (2015) that degradation is a state of arrested succession.

Thus far, mostly negative effects of *Dicranopteris* have been discussed. However, it can improve seedling survival of certain species on landslides providing shade and improving soil parameters, such as an increase in N (Walker 1994). Some say it can prevent soil erosion (Holttum 1959; Yang L et al. 2020) and Zhao et al. (2012) showed that the removal of *Dicranopteris dichotoma* in the understory reduced soil biota abundance and litter decomposition rates, which indicates its importance to the ecosystem. However, Wyns (2015) showed that respiration rates in *D. pectinata* litter layer was lower than in adjacent forests and questioned a long-term stabilizing effect on soils as its root system is often very shallow.

Utilizing *Dicranopteris* could change the perspective on the thickets. Traditional uses include medicine (Zakaria et al. 2006), fish-traps and pens (Holttum 1959) made out of *Dicranopteris*, which all have a more modern counterpart. More modern uses could

come from the ferns being hyperaccumulators, i.e. plants that accumulate large amounts of metals in their aboveground organs (Rascio and Navari-Izzo 2011). For instance, Jally et al. (2021) extracted a solution containing 74 % of rare earth elements from *D. linearis* occurring naturally in former mining sites, indicating the potential for phytomining. Wei et al. (2020) showed favourable effects from ashes of *D. pedata* on the growth of water spinach, indicating the potential as fertilizer. Similar studies on *Dicranopteris pectinata* would be interesting.

For now, the most viable option in dealing with the fern in the vicinity of La Gamba seems to be clearing the sites to promote forest regeneration. The most common practice to eradicate *Dicranopteris* thickets in Costa Rica is through burning (Wyns 2015). Ainsworth and Kauffman (2010) showed that *Dicranopteris linearis* slowly recolonized sites from adjacent patches after fire in Hawaii. However, Sohng et al. (2017) reported fire facilitating *Dicranopteris linearis* in Sri Lanka by killing most of the other plants and surviving plants quickly being shaded out due to the fern's growth pattern. Therefore, mechanical removal could be favourable, albeit hard labour. Slocum et al. (2006) showed that mechanical clearing of *D. pectinata* and planting trees in clearings could prove successful in countering the fern's dominance and promote natural regeneration in Puerto Rico. Animals play an important role in seed dispersal of plant species in neotropical forests (Willson et al. 1989; Wunderle 1997). Given the lack of natural perches in *Dicranopteris* patches, the thickets might not be attractive to birds which results in fewer bird dispersed seeds (Shiels and Walker 2003). Holl (1998) showed that implementing bird perches on agricultural lands of Costa Rica led to a significant increase in bird dispersed seeds. Similarly, Shiels and Walker (2003) showed more bird dispersed seeds on landslides with perches than on landslides without perches. Some of the landslides were covered by *Dicranopteris*. Therefore, setting up perches could be a cost-efficient and easy method to aid natural regeneration on fern-dominated sites, though the fern probably has to be removed before for the method to be effective.

4.6 Conclusion

Dicranopteris pectinata arrests the succession in the vicinity of La Gamba. Remote sensing data, including drone campaigns and classifications can be a useful tool to monitor and estimate the persistence of the thickets, though some background knowledge is required and ground truthing is recommended. As such, a persistent state of several decades could be proven. Comparing images of different times and spatial resolution can be difficult. Semi-automatic classifications rely on a sufficient input of good quality to deliver a satisfying result. The comparison of classifications with differing accuracies can lead to false results. Extrapolating the results of the classification more than 1 % of the whole area are covered in fern, which results in a significantly lower biomass accumulation than in areas regenerating to forests.

The most viable management option in the vicinity of La Gamba may be the periodic mechanical removal of fern thickets and sowing seeds in the clearings. Bird perches are a cheap and easy method that can increase the attractivity for seed dispersers, thus they should be incorporated. These efforts should be particularly focused on slopes, as *Dicranopteris* seems to outcompete trees on these sites more.

Acknowledgements

I would like to express my gratitude to everybody who contributed to the creation of this study, without whom my endeavours would not have been possible.

Thank you to my supervisor Peter Hietz, for giving me the unique opportunity to conduct research in the beautiful tropical rainforest of Costa Rica. For helping me get accustomed to the new environment in the early days of the trip, for all the insights and comments and your help with acquiring the drone and satellite image.

Thank you to my co-supervisor Markus Immitzer, for all the advice and comments not only on the remote sensing part of this work, despite asking for it on short notice. Also, thanks for your help with acquiring satellite imagery, in particular the PlanetScope scenes.

Thanks to Reinfried Mansberger, for the advice and insights on the photogrammetry part of this study.

Thank you to KUWI and Rainforest Luxembourg for the financial support.

Thanks to Planet's Education and Research (E&R) Program for providing the PlanetScope scenes.

Erika Coelho Veiga, you have contributed so much, I don't even know where to begin. Thanks for assisting me with some of the field work, all the translations, in particular to unlock no-fly areas, and all the proof reading and notes on the thesis. Thank you so much for being by my side, helping me maintain my composure and focus.

Thanks to everyone at the Tropical Field Station La Gamba and COBIGA, for being so accommodating. Special thanks to Jacob and Luís for helping me to get the approval of landowners to work on their premises. Thanks to all the landowners allowing me to work on their properties.

Thank you to my parents for the support throughout my studies.

Thanks to every guest of the station for making this trip more memorable.

Image References

Figure 1: Houghton R. 2012. Carbon emissions and the drivers of deforestation and forest degradation in the tropics. *Current Opinion in Environmental Sustainability*. 4(6):597–603. doi:10.1016/j.cosust.2012.06.006.

Figure 3: POWO. 2022 *Gleichenella pectinata* (Willd.) Ching. <https://powo.science.kew.org/taxon/urn:lsid:ipni.org:names:110733-2/>. Last accessed 17/01/2023.

Figure 4: Tropenstation La Gamba. 2020 Wissenschaftliche Informationen zur Region Golfo Dulce, Klima. <https://www.lagamba.at/forschung/wissenschaftliche-informationen/>. Last accessed 17/01/2023.

Figures 5 & 10: Google Earth. 05.03.2015 La Gamba, Costa Rica. © 2022 CNES / Airbus.

Figure 8: Aerotas. n.d. Overlap & Flight pattern – Flight Plan best practices. <https://www.aerotas.com/overlap-flight-pattern>. Last accessed 23/10/2022

Figure 11: Congedo L. 2021. Semi-Automatic Classification Plugin: A Python tool for the download and processing of remote sensing images in QGIS. *JOSS*. 6(64):3172. doi:10.21105/joss.03172.

References

- Acácio V, Holmgren M, Jansen PA, Schrotter O. 2007. Multiple Recruitment Limitation Causes Arrested Succession in Mediterranean Cork Oak Systems. *Ecosystems*. 10(7):1220–1230. doi:10.1007/s10021-007-9089-9.
- Ainsworth A, Kauffman JB. 2010. Interactions of Fire and Nonnative Species Across an Elevation/Plant Community Gradient in Hawaii Volcanoes National Park. *Biotropica*. 42(6):647–655. doi:10.1111/j.1744-7429.2010.00636.x.
- Amatangelo KL, Vitousek PM. 2009. Contrasting Predictors of Fern versus Angiosperm Decomposition in a Common Garden. *Biotropica*. 41(2):154–161. doi:10.1111/j.1744-7429.2008.00470.x.
- Anderson-Teixeira KJ, Wang MMH, McGarvey JC, LeBauer DS. 2016. Carbon dynamics of mature and regrowth tropical forests derived from a pantropical database (TropForC-db). *Glob Chang Biol*. 22(5):1690–1709. eng. doi:10.1111/gcb.13226.
- Ashton MS, Gunatilleke CVS, Singhakumara BMP, Gunatilleke, I A U N. 2001. Restoration pathways for rain forest in southwest Sri Lanka: a review of concepts and models. *Forest Ecology and Management*. 154(3):409–430. doi:10.1016/S0378-1127(01)00512-6.
- Bennet L. 2017. Deforestation and Climate Change. Washington: Climate Institute; [accessed 2022 Nov 15]. https://climate.org/wp-content/uploads/2017/04/deforestation-final_r1.pdf.
- Boyes LJ, Gunton RM, Griffiths ME, Lawes MJ. 2011. Causes of arrested succession in coastal dune forest. *Plant Ecol*. 212(1):21–32. doi:10.1007/s11258-010-9798-6.
- Chapin FS, Matson PA, Mooney HA. 2002. Principles of terrestrial ecosystem ecology. New York, Berlin, Heidelberg: Springer. 436 p. ISBN: 0-387-95439-2. eng. <http://www.loc.gov/catdir/enhancements/fy0817/2002017654-d.html>.
- Chau NL, Chu LM. 2017. Fern cover and the importance of plant traits in reducing erosion on steep soil slopes. *CATENA*. 151:98–106. doi:10.1016/j.catena.2016.12.016.
- Chazdon RL, Broadbent EN, Rozendaal DMA, Bongers F, Zambrano AMA, Aide TM, Balvanera P, Becknell JM, Boukili V, Brancalion PHS, et al. 2016. Carbon sequestration potential of second-growth forest regeneration in the Latin American tropics. *Sci Adv*. 2(5):e1501639. eng. doi:10.1126/sciadv.1501639.
- Chua SC, Ramage BS, Potts MD. 2016. Soil degradation and feedback processes affect long-term recovery of tropical secondary forests. *J Veg Sci*. 27(4):800–811. doi:10.1111/jvs.12406.

- Congedo L. 2021. Semi-Automatic Classification Plugin: A Python tool for the download and processing of remote sensing images in QGIS. *JOSS*. 6(64):3172. doi:10.21105/joss.03172.
- Corlett R, Primack RB. 2011. *Tropical rain forests: An ecological and biogeographical comparison*. 2. ed. Chichester: Wiley-Blackwell. 326 p. ISBN: 978-1-4443-3254-4. eng.
- Crausbay SD, Martin PH. 2016. Natural disturbance, vegetation patterns and ecological dynamics in tropical montane forests. *J. Trop. Ecol.* 32(5):384–403. doi:10.1017/S0266467416000328.
- DeSoto L, Olano JM, Rozas V, La Cruz M de. 2010. Release of *Juniperus thurifera* woodlands from herbivore-mediated arrested succession in Spain. *Applied Vegetation Science*. 13(1):15–25. doi:10.1111/j.1654-109X.2009.01045.x.
- DJI. 2021. *DJI MINI 2: Benutzerhandbuch v.1.4 2021.06.*: [accessed 2023 Jan 14]. https://dl.djicdn.com/downloads/DJI_Mini_2/20210630/DJI_Mini_2_User_Manual_DE.pdf.
- Dos Santos EPG, Lehmann DRM, Santos M, Randi ÁM. 2010. Spore germination of *Gleichenella pectinata* (Willd.) Ching (Polypodiopsida-Gleicheniaceae) at different temperatures, levels of light and pH. *Braz. arch. biol. technol.* 53(6):1309–1318. doi:10.1590/S1516-89132010000600007.
- Eisenbeiss H, Sauerbier M. 2019. Data acquisition and Mapping. In: Armenakis C, Patias P, editors. *Unmanned vehicle systems for geomatics: Towards robotic mapping*. Dunbeath: Whittles Publishing. p. 176–193.
- ESA. 2023a. PlanetScope.: ESA; [accessed 2023 Feb 18]. <https://earth.esa.int/eogateway/missions/planetscope>.
- ESA. 2023b. Pleiades.: ESA; [accessed 2023 Feb 18]. <https://earth.esa.int/eogateway/missions/pleiades>.
- Fagan ME, DeFries RS, Sesnie SE, Arroyo-Mora JP, Chazdon RL. 2016. Targeted reforestation could reverse declines in connectivity for understory birds in a tropical habitat corridor. *Ecol Appl.* 26(5):1456–1474. eng. doi:10.1890/14-2188.
- FAO. 2002a. *Proceedings: Expert meeting on harmonizing forest-related definitions for use by various stakeholders [Rome, 22-25 January 2002].*: [accessed 2023 Jan 13]. <https://www.fao.org/forestry/15533-0cb816e82c09c14873ce9226dd13910b9.pdf>.
- FAO. 2002b. *Proceedings: second expert meeting on harmonizing forest-related definitions for use by various stakeholders. [11-13 September 2002]. Rome;* [accessed 2023 Jan 13]. <https://www.fao.org/forestry/10803-056b14a3d809baaa81fc6a6d868f62e3a.pdf>.

- FAO. 2020. Global forest resources assessment 2020: Main report. 2nd edition. Rome: Food & Agriculture Organization of the UN. 179 p. ISBN: 978-92-5-132974-0.
- FAO. 2022. The State of the World's Forests 2022.: FAO. ISBN: 978-92-5-135984-6.
- Finegan B. 1996. Pattern and process in neotropical secondary rain forests: the first 100 years of succession. *Trends Ecol Evol.* 11(3):119–124. doi:10.1016/0169-5347(96)81090-1.
- Forlani G, Dall'Asta E, Diotri F, Di Cella UM, Roncella R, Santise M. 2018. Quality Assessment of DSMs Produced from UAV Flights Georeferenced with On-Board RTK Positioning. *Remote Sensing.* 10(2):311. doi:10.3390/rs10020311.
- Ghazoul J, Burivalova Z, Garcia-Ulloa J, King LA. 2015. Conceptualizing Forest Degradation. *Trends Ecol Evol.* 30(10):622–632. eng. doi:10.1016/j.tree.2015.08.001.
- Ghazoul J, Chazdon R. 2017. Degradation and Recovery in Changing Forest Landscapes: A Multiscale Conceptual Framework. *Annu. Rev. Environ. Resour.* 42(1):161–188. doi:10.1146/annurev-environ-102016-060736.
- Goldsmith GR, Comita LS, Chua SC. 2011. Evidence for arrested succession within a tropical forest fragment in Singapore. *J. Trop. Ecol.* 27(03):323–326. doi:10.1017/S0266467411000010.
- Gul J, Zhang Y, Liu Q. 2019. Allelopathic effects of native plant species *Dicranopteris dichotoma* on invasive species *Bidens pilosa* and *Eupatorium catarium*. *AJ.* 48(1):45–58. doi:10.26651/allelo.j/2019-48-1-1243.
- Heinrich K, Buchroithner M, Bender O. 2009. The use of satellite remote sensing for the detection and analysis of geocultural heritages. In: Bender O, Evelpidou N, Krek A, Vassilopoulos A, editors. *Geoinformation technologies for geocultural landscapes: European perspectives*. Boca Raton, London, New York, Leiden: CRC Press Taylor & Francis Group. p. 67–86.
- Heipke C, Freeden W, Rummel R, editors. 2017. *Photogrammetrie und Fernerkundung*. 1. Auflage. Berlin: Springer Spektrum. 839 p. (Springer Reference Naturwissenschaften). ISBN: 978-3-662-47093-0. ger.
- Holl KD. 1998. Do Bird Perching Structures Elevate Seed Rain and Seedling Establishment in Abandoned Tropical Pasture? *Restor Ecology.* 6(3):253–261. doi:10.1046/j.1526-100X.1998.00638.x.
- Holttum R. 1959. Gleicheniaceae. *Flora Malesiana.* 2, Pteridophyta(1):1–36.
- Houghton R. 2012. Carbon emissions and the drivers of deforestation and forest degradation in the tropics. *Current Opinion in Environmental Sustainability.* 4(6):597–603. doi:10.1016/j.cosust.2012.06.006.

- Hughes RF, Asner GP, Mascaro J, Uowolo A, Baldwin J. 2014. Carbon storage landscapes of lowland Hawaii: the role of native and invasive species through space and time. *Ecol Appl.* 24(4):716–731. eng. doi:10.1890/12-2253.1.
- Inderjit, Mallik A. 2002. Can *Kalmia angustifolia* interference to black spruce (*Picea mariana*) be explained by allelopathy? *Forest Ecology and Management.* 160(1-3):75–84. doi:10.1016/S0378-1127(01)00463-7.
- Jally B, Laubie B, Chour Z, Muhr L, Qiu R, Morel JL, Tang Y, Simonnot M-O. 2021. A new method for recovering rare earth elements from the hyperaccumulating fern *Dicranopteris linearis* from China. *Minerals Engineering.* 166:106879. doi:10.1016/j.mineng.2021.106879.
- Jensen JR, Im J, Hardin P, Jensen RR. 2008. Image Classification. In: *The SAGE handbook of remote sensing.* Online-Ausg. Thousand Oaks, Calif, London: SAGE. p. 269–281.
- Johnston E. 2022. Costa Rica: Paradise on Earth: How is this small country home to such a wealth of wildlife?: Royal Botanical Gardens Kew; [updated 2022 Feb 16; accessed 2022 Nov 13]. <https://www.kew.org/read-and-watch/costa-rica-biodiversity>.
- Kato-Noguchi H, Saito Y, Suenaga K. 2012. Involvement of allelopathy in the establishment of pure colony of *Dicranopteris linearis*. *Plant Ecol.* 213(12):1937–1944. doi:10.1007/s11258-012-0096-3.
- Kellermann B, Lacerda AEB. 2019. Arrested development? Investigating the role of bamboo in *Araucaria* Forest succession in Southern Brazil. *Journal of Plant Ecology.* doi:10.1093/jpe/rtz037.
- Kitayama K, Mueller-Dombois D, Vitousek PM. 1995. Primary succession of Hawaiian montane rain forest on a chronosequence of eight lava flows. *Journal of Vegetation Science.* 6(2):211–222. doi:10.2307/3236216.
- Kneller M. 2009. Pollen Analysis. In: Gornitz V, editor. *Encyclopedia of Paleoclimatology and Ancient Environments.* Dordrecht: Springer Netherlands. p. 815–823 (*Encyclopedia of Earth Sciences Series*).
- Kratochwil A, Schwabe A. 2001. *Ökologie der Lebensgemeinschaften: Biozöologie.* Stuttgart: Ulmer. 756 p. (UTB für Wissenschaft Biologie, Ökologie, Agrar-, Forst- und Geowissenschaften, Landschaftsplanung; vol. 8199). ISBN: 3-8252-8199-X. ger.
- Kricher JC. 2011. *Tropical ecology.* Princeton, N.J.: Princeton University Press. 632 p. ISBN: 978-0-691-11513-9. eng.
- Kuroda A, Mukai S, Toyohara G. 2006. Floristic composition and community structure of dense undergrowth vegetation formed by evergreen perennial ferns,

- Dicranopteris linearis and Gleichenia japonica (Gleicheniaceae). *Vegetation Science*. 23(1):25–36.
- Lamb D. 2011. *Regreening the Bare Hills*. Dordrecht: Springer Netherlands (vol. 8). ISBN: 978-90-481-9869-6.
- Letcher SG, Chazdon RL. 2009. Rapid Recovery of Biomass, Species Richness, and Species Composition in a Forest Chronosequence in Northeastern Costa Rica. *Biotropica*. 41(5):608–617. doi:10.1111/j.1744-7429.2009.00517.x.
- Levy-Tacher S, Vleut I, Román-Dañobeytia F, Aronson J. 2015. Natural Regeneration after Long-Term Bracken Fern Control with Balsa (*Ochroma pyramidale*) in the Neotropics. *Forests*. 6(12):2163–2177. doi:10.3390/f6062163.
- Liang S, editor. 2012. *Advanced remote sensing: Terrestrial information extraction and applications*. 1. ed. Amsterdam, Heidelberg: Elsevier Acad. Press. 799 p. ISBN: 978-0-12-385954-9. eng.
- Lima LV, Oliveira Dittrich VA de, Souza FC, Da Fonseca CR, Salino A. 2021. FRAGMENTED BIODIVERSITY: FERNS AND LYCOPHYTES FROM FOREST FRAGMENTS IN JUIZ DE FORA, MINAS GERAIS, BRAZIL.
- Li-Ping L, Gang G, Yong T, Ju-Xin Y. 1999. The Allelopathy of the Extract from *Dicranopteris pedata* on Several Weeds and Crops. *Chinese Bulletin of Botany*. 16(05):591–597.
- Lo M, Reed J, Castello L, Steel EA, Frimpong EA, Ickowitz A. 2020. The Influence of Forests on Freshwater Fish in the Tropics: A Systematic Review. *Bioscience*. 70(5):404–414. eng. doi:10.1093/biosci/biaa021.
- Locatelli B, Catterall CP, Imbach P, Kumar C, Lasco R, Marín-Spiotta E, Mercer B, Powers JS, Schwartz NB, Uriarte M. 2015. Tropical reforestation and climate change: beyond carbon. *Restor Ecology*. 23(4):337–343. doi:10.1111/rec.12209.
- MacCaughey V. 1918. THE GENUS GLEICHENIA (DICRANOPTERIS) IN THE HAWAIIAN ISLANDS. *Torreyana*. 18(3):41–52.
- Martin PH, Fahey TJ, Sherman RE. 2011. Vegetation Zonation in a Neotropical Montane Forest: Environment, Disturbance and Ecotones. *Biotropica*. 43(5):533–543. doi:10.1111/j.1744-7429.2010.00735.x.
- McCann JA, Keith DA, Kingsford RT. 2022. Measuring plant biomass remotely using drones in arid landscapes. *Ecol Evol*. 12(5):e8891. eng. doi:10.1002/ece3.8891.
- McFarland BJ. 2018. The Context of Tropical Rainforest Deforestation and Degradation. In: McFarland BJ, editor. *Conservation of Tropical Rainforests*. Cham: Springer International Publishing. p. 7–58.
- Mitchell AL, Rosenqvist A, Mora B. 2017. Current remote sensing approaches to monitoring forest degradation in support of countries measurement, reporting and

- verification (MRV) systems for REDD. *Carbon Balance Manag.* 12(1):9. eng. doi:10.1186/s13021-017-0078-9.
- Mueller-Dombois D, Boehmer HJ. 2013. Origin of the Hawaiian rainforest and its transition states in long-term primary succession. *Biogeosciences.* 10(7):5171–5182. doi:10.5194/bg-10-5171-2013.
- Oberleitner F, Egger C, Oberdorfer S, Dullinger S, Wanek W, Hietz P. 2021. Recovery of aboveground biomass, species richness and composition in tropical secondary forests in SW Costa Rica. *Forest Ecology and Management.* 479:118580. doi:10.1016/j.foreco.2020.118580.
- Phillips, Malhi, Higuchi, Laurance, Nunez, Vasquez, Ferreira, Stern, Brown, Grace. 1998. Changes in the carbon balance of tropical forests: evidence from long-term plots. *Science.* 282(5388):439–442. eng. doi:10.1126/science.282.5388.439.
- Planet. 2023. Norway's International Climate and Forests Initiative Satellite Data Program.: [accessed 2023 Jan 13]. <https://www.planet.com/nicfi/>.
- Planet Team. 2022. Planet Application Program Interface: In Space for Life on Earth. San Francisco, CA.: <https://api.planet.com/>.
- Poorter L, Bongers F, Aide TM, Almeyda Zambrano AM, Balvanera P, Becknell JM, Boukili V, Brancalion PHS, Broadbent EN, Chazdon RL, et al. 2016. Biomass resilience of Neotropical secondary forests. *Nature.* 530(7589):211–214. eng. doi:10.1038/nature16512.
- Poorter L, van der Sande MT, Thompson J, Arets EJMM, Alarcón A, Álvarez-Sánchez J, Ascarrunz N, Balvanera P, Barajas-Guzmán G, Boit A, et al. 2015. Diversity enhances carbon storage in tropical forests. *Global Ecology and Biogeography.* 24(11):1314–1328. doi:10.1111/geb.12364.
- POWO. 2022. Plants of the World Online [Facilitated by the Royal Botanic Gardens, Kew. Published on the Internet].: [accessed 2022 Nov 28]. <http://www.plantsoftheworldonline.org/>.
- Propeller Aero. 2021. What is Ground Sample Distance (GSD) and How Does it Affect Your Drone Data?: [updated 2021 May 30; accessed 2023 Jan 15]. <https://www.propelleraero.com/blog/ground-sample-distance-gsd-calculate-drone-data/>.
- Rascio N, Navari-Izzo F. 2011. Heavy metal hyperaccumulating plants: how and why do they do it? And what makes them so interesting? *Plant Sci.* 180(2):169–181. eng. doi:10.1016/j.plantsci.2010.08.016.
- Resnik B, Bill R. 2009. Vermessungskunde für den Planungs-, Bau- und Umweltbereich. 3., neu bearb. und erw. Aufl. Heidelberg, München, Landsberg, Frechen, Hamburg: Wichmann. 329 p. ISBN: 978-3-87907-488-4. ger.

- Royo AA, Carson WP. 2006. On the formation of dense understory layers in forests worldwide: consequences and implications for forest dynamics, biodiversity, and succession. *Can. J. For. Res.* 36(6):1345–1362. doi:10.1139/x06-025.
- Russell AE, Raich JW, Vitousek PM. 1998. The ecology of the climbing fern *Dicranopteris linearis* on windward Mauna Loa, Hawaii. *J Ecology.* 86(5):765–779. doi:10.1046/j.1365-2745.1998.8650765.x.
- Russell AE, Vitousek PM. 1997. Decomposition and potential nitrogen fixation in *Dicranopteris linearis* litter on Mauna Loa, Hawai'i. *J. Trop. Ecol.* 13(4):579–594. doi:10.1017/S0266467400010737.
- Salim HL, Adi NS, Kepel TL, Ati RNA. 2020. Estimating mangrove biomass using drone in Karimunjawa Islands. *IOP Conf. Ser.: Earth Environ. Sci.* 561(1):12054. doi:10.1088/1755-1315/561/1/012054.
- Schaefer M. 2012. Wörterbuch der Ökologie. 5. neu bearbeitete und erweiterte Auflage. Heidelberg: Spektrum Akademischer Verlag. 379 p. ISBN: 978-3-8274-2561-4. ger.
- Schnitzer N. 2014. From a Pasture to Rainforest : Performance of Native Tree Species in Ecological Restoration of Tropical Lowland Rainforest, Costa Rica (Case Study) [Master Thesis]. Vienna: University of Life Sciences and Natural Resources, Botany.
- Schultz J. 2000. Handbuch der Ökozonen. Stuttgart: Ulmer. 577 p. (UTB für Wissenschaft Geographie, Ökologie, Agrar- und Forstwissenschaften; vol. 8200). ISBN: 3-8252-8200-7. ger.
- Shiels AB, Walker LR. 2003. Bird Perches Increase Forest Seeds on Puerto Rican Landslides. *Restor Ecology.* 11(4):457–465. doi:10.1046/j.1526-100X.2003.rec0269.x.
- Shono K, Davies SJ, Chua YK. 2007. PERFORMANCE OF 45 NATIVE TREE SPECIES ON DEGRADED LANDS IN SINGAPORE. *Journal of Tropical Forest Science.* 19(1):25–34.
- Shono K, Davies SJ, Kheng CY. 2006. Regeneration of native plant species in restored forests on degraded lands in Singapore. *Forest Ecology and Management.* 237(1-3):574–582. doi:10.1016/j.foreco.2006.10.003.
- Slocum MG, Aide TM, Zimmerman JK, Navarro L. 2004. Natural regeneration of subtropical montane forest after clearing fern thickets in the Dominican Republic. *J. Trop. Ecol.* 20(4):483–486. doi:10.1017/S0266467404001646.
- Slocum MG, Mitchell Aide T, Zimmerman JK, Navarro L. 2006. A Strategy for Restoration of Montane Forest in Anthropogenic Fern Thickets in the Dominican Republic. *Restor Ecology.* 14(4):526–536. doi:10.1111/j.1526-100X.2006.00164.x.

- Sohng J, Singhakumara BM, Ashton MS. 2017. Effects on soil chemistry of tropical deforestation for agriculture and subsequent reforestation with special reference to changes in carbon and nitrogen. *Forest Ecology and Management*. 389:331–340. doi:10.1016/j.foreco.2016.12.013.
- Spracklen DV, Baker J, Garcia-Carreras L, Marsham JH. 2018. The Effects of Tropical Vegetation on Rainfall. *Annu. Rev. Environ. Resour.* 43(1):193–218. doi:10.1146/annurev-environ-102017-030136.
- Takehige R, Onishi M, Aoyagi R, Sawada Y, Imai N, Ong R, Kitayama K. 2022. Mapping the Spatial Distribution of Fern Thickets and Vine-Laden Forests in the Landscape of Bornean Logged-Over Tropical Secondary Rainforests. *Remote Sensing*. 14(14):3354. doi:10.3390/rs14143354.
- Tet-Vun C, Ismail B. 2006. Field evidence of the allelopathic properties of *Dicranopteris linearis*. *Weed Biol Manage.* 6(2):59–67. doi:10.1111/j.1445-6664.2006.00203.x.
- Thrippleton T, Bugmann H, Snell RS. 2018. Herbaceous competition and browsing may induce arrested succession in central European forests. *J Ecology*. 106(3):1120–1132. doi:10.1111/1365-2745.12889.
- Turner IM. 2001. Rainforest Ecosystems, Plant Diversity. In: *Encyclopedia of Biodiversity*.: Elsevier. p. 13–23.
- Underwood LM. 1907. American Ferns-VIII. A Preliminary Review of the North American Gleicheniaceae. *Bulletin of the Torrey Botanical Club*. 34(5):243. doi:10.2307/2560334.
- Vitousek PM, Tweiten MA, Kellner J, Hotchkiss SC, Chadwick OA, Asner GP. 2010. Top-Down Analysis of Forest Structure and Biogeochemistry Across Hawaiian Landscapes. *Pacific Science*. 64(3):359–366. doi:10.2984/64.3.359.
- Walker LR. 1994. Effects of fern thickets on woodland development on landslides in Puerto Rico. *Journal of Vegetation Science*. 5(4):525–532. doi:10.2307/3235979.
- Walker LR, Boneta W. 1995. Plant and soil responses to fire on a fern-covered landslide in Puerto Rico. *J. Trop. Ecol.* 11(3):473–479. doi:10.1017/S0266467400008981.
- Walker LR, Landau FH, Velázquez E, Shiels AB, Sparrow AD. 2010. Early successional woody plants facilitate and ferns inhibit forest development on Puerto Rican landslides. *J Ecology*. 98(3):625–635. doi:10.1111/j.1365-2745.2010.01641.x.
- Walker LR, Shiels AB, Bellingham PJ, Sparrow AD, Fetcher N, Landau FH, Lodge DJ. 2013. Changes in abiotic influences on seed plants and ferns during 18 years of primary succession on Puerto Rican landslides. *J Ecology*. 101(3):650–661. doi:10.1111/1365-2745.12071.

- Wei Z, Gao B, Cheng KY, Kaksonen AH, Kolev SD, Wong JWC, Cui J. 2020. Exploring the use of *Dicranopteris pedata* ash as a rare earth fertilizer to *Ipomoea aquatica* Forsskal. *J Hazard Mater.* 400:123207. eng. doi:10.1016/j.jhazmat.2020.123207.
- Weih RC, Riggan ND. 2010. Object-based classification vs. pixel-based classification: Comparative importance of multi-resolution imagery. *The International Archives of the Photogrammetry, Remote Sensing and Spatial Information Sciences*; [accessed 2023 Mar 1]. (Vol. XXXVIII-4/C7). https://www.isprs.org/proceedings/xxxviii/4-c7/pdf/Weih_81.pdf.
- Weissenhofer A, Huber W, Zamora N, Weber A, González J. 2001. A Brief Outline of the Flora and Vegetation of the Golfo Dulce Region. In: Biologiezentrum des OÖ Landesmuseums, editor. An introductory field guide to the flowering plants of the Golfo Dulce rain forests Costa Rica: Corcovado National Park and Piedras Blancas National Park ("Regenwald der Österreicher"). Linz: OÖ. Landesmuseum. p. 15–24 (Catalogue of OÖ. Landesmuseums; N.F. 172).
- Weissenhofer A, Jenking D, Huber W. 2016. Der Biologische Korridor COBIGA in La Gamba: Corredor Biológico La Gamba, Regenwald der Österreicher, Costa Rica. *ÖKO-L.* 38(3):16–26.
- Wheeler CE, Omeja PA, Chapman CA, Glipin M, Tumwesigye C, Lewis SL. 2016. Carbon sequestration and biodiversity following 18 years of active tropical forest restoration. *Forest Ecology and Management.* 373:44–55. doi:10.1016/j.foreco.2016.04.025.
- Willson MF, Irvine AK, Walsh NG. 1989. Vertebrate Dispersal Syndromes in Some Australian and New Zealand Plant Communities, with Geographic Comparisons. *Biotropica.* 21(2):133. doi:10.2307/2388704.
- Wunderle JM. 1997. The role of animal seed dispersal in accelerating native forest regeneration on degraded tropical lands. *Forest Ecology and Management.* 99(1-2):223–235. doi:10.1016/S0378-1127(97)00208-9.
- Wyns A. 2015. Arrested succession in Costa Rican lowland secondary rainforest through a *Dicranopteris pectinata* understory [Master's thesis]. Brussels: Vrije Universiteit Brussel, Plant Biology and Nature Management.
- Yamagawa H, Ito S, Nakao T. 2010. Restoration of semi-natural forest after clearcutting of conifer plantations in Japan. *Landscape Ecol Eng.* 6(1):109–117. doi:10.1007/s11355-009-0088-1.
- Yang L, Huang Y, Lima LV, Sun Z, Liu M, Wang J, Liu N, Ren H. 2020. Rethinking the Ecosystem Functions of *Dicranopteris*, a Widespread Genus of Ferns. *Front Plant Sci.* 11:581513. eng. doi:10.3389/fpls.2020.581513.

- Zakaria ZA, Abdul Ghani ZDF, Raden Mohd Nor RNS, Gopalan HK, Sulaiman MR, Abdullah FC. 2006. Antinociceptive and anti-inflammatory activities of *Dicranopteris linearis* leaves chloroform extract in experimental animals. *Yakugaku Zasshi*. 126(11):1197–1203. eng. doi:10.1248/yakushi.126.1197.
- Zaman K. 2022. Environmental cost of deforestation in Brazil's Amazon Rainforest: Controlling biocapacity deficit and renewable wastes for conserving forest resources. *Forest Ecology and Management*. 504:119854. doi:10.1016/j.foreco.2021.119854.
- Zhao J, Wan S, Li Z, Shao Y, Xu G, Liu Z, Zhou L, Fu S. 2012. *Dicranopteris*-dominated understory as major driver of intensive forest ecosystem in humid subtropical and tropical region. *Soil Biology and Biochemistry*. 49:78–87. doi:10.1016/j.soilbio.2012.02.020.

Appendix

Table 3: Manually assessed fern-dominated area for all years and plots.

Manually assessed fern-dominated area			
Plot	Drone images '22 [m ²]	PlanetScope scene '22 [m ²]	PlanetScope scene '17 [m ²]
1	6593	4235	4754
2	6317	5231	3300
3	2761	1920	1898
6	4887	2608	2315
7	2895	1350	1742
8	4100	4361	1769
9	10277	6740	2961
10	16627	13266	6902
11	29774	20237	8935
12	15465	14364	5027
13	38900	28624	10559
14	22705	16293	8811
15	6130	3529	518
16	1881	1404	747
17	15443	12944	5669
18	4068	3704	1090
19	266	175	0
20	2997	2307	304
21	23004	18861	16051
22	11927	4852	2890
23	4244	2318	1773
24	3682	3788	3722
25	6293	2414	1187

Plot	Pléiades scene '15 [m ²]	Aerial photography '98 [m ²]
1	5894	NA
2	4808	NA
3	2125	NA
6	2918	NA
7	3944	NA
8	1808	NA
9	7168	NA
10	14312	NA
11	15242	NA
12	10581	NA
13	20132	NA
14	17392	2788
15	3889	NA
16	411	NA
17	11433	NA
18	1231	NA
19	0	0
20	933	0
21	18703	8420
22	7234	NA
23	3077	NA
24	3743	NA
25	2737	NA

Table 4: Fern-dominated area for each year and plot according to the semi-automatic classifications.

Semi-automatically assessed areas		
Plot	First PlanetScope '22 [m ²]	Second Planetscope '22 [m ²]
1	3717	3456
2	4158	4302
3	1503	1350
6	1566	1674
7	900	909
8	5202	5076
9	4392	5184
10	10206	10377
11	22869	21105
12	15389	14624
13	19090	21475
14	8784	10017
15	135	684
16	981	918
17	9549	9342
18	1575	1773
19	0	0
20	0	144
21	12609	10908
22	891	1323
23	1413	1269
24	3285	3024
25	945	1080
Plot	PlanetScope scene '17 [m ²]	Pléiades scene '15[m ²]
1	3987	6739
2	3726	4641
3	1422	3127
6	2058	3681
7	891	3220
8	8010	2137
9	1602	6857
10	7209	10667
11	16155	10964
12	1024	14225
13	15703	20907
14	6534	13241
15	27	1838
16	459	1174
17	8928	12908
18	747	1524
19	0	0
20	0	870
21	12654	19636
22	198	7529
23	1989	3615
24	3762	4702
25	837	3864

Table 5: Overview over all classified land cover classes for each year and classification.

	PlanetScope '22 first classification [ha]	PlanetScope '22 second classification [ha]
Forest	11061,8973	11702,3652
Fern	176,4954	150,66
Agriculture	2916,3339	2399,3505
Settlement	290,6703	187,2351
Water	816,0489	110,7702
Clouds	0	711,0648
Total	15261,4458	15261,4458
	PlanetScope '17 [ha]	Pléiades '15 [ha]
Forest	9833,3028	10361,3303
Fern	66,0879	1714,3624
Agriculture	2801,9934	3369,3542
Settlement	144,9936	130,016
Water	50,7267	74,9571
Clouds	279,5553	76,1136
Total	13176,6597	15726,1336